AD-A047 197 GENERAL ELECTRIC CO PHILADELPHIA PA SPACE DIV F/G 20/5
LOW REPETITION RATE COPPER VAPOR LASER.(U)
SEP 77 R S ANDERSON, R J HOMSEY, T W KARRAS N00014-76-C-0975
UNCLASSIFIED NL

1 OF 2
AD
A047197

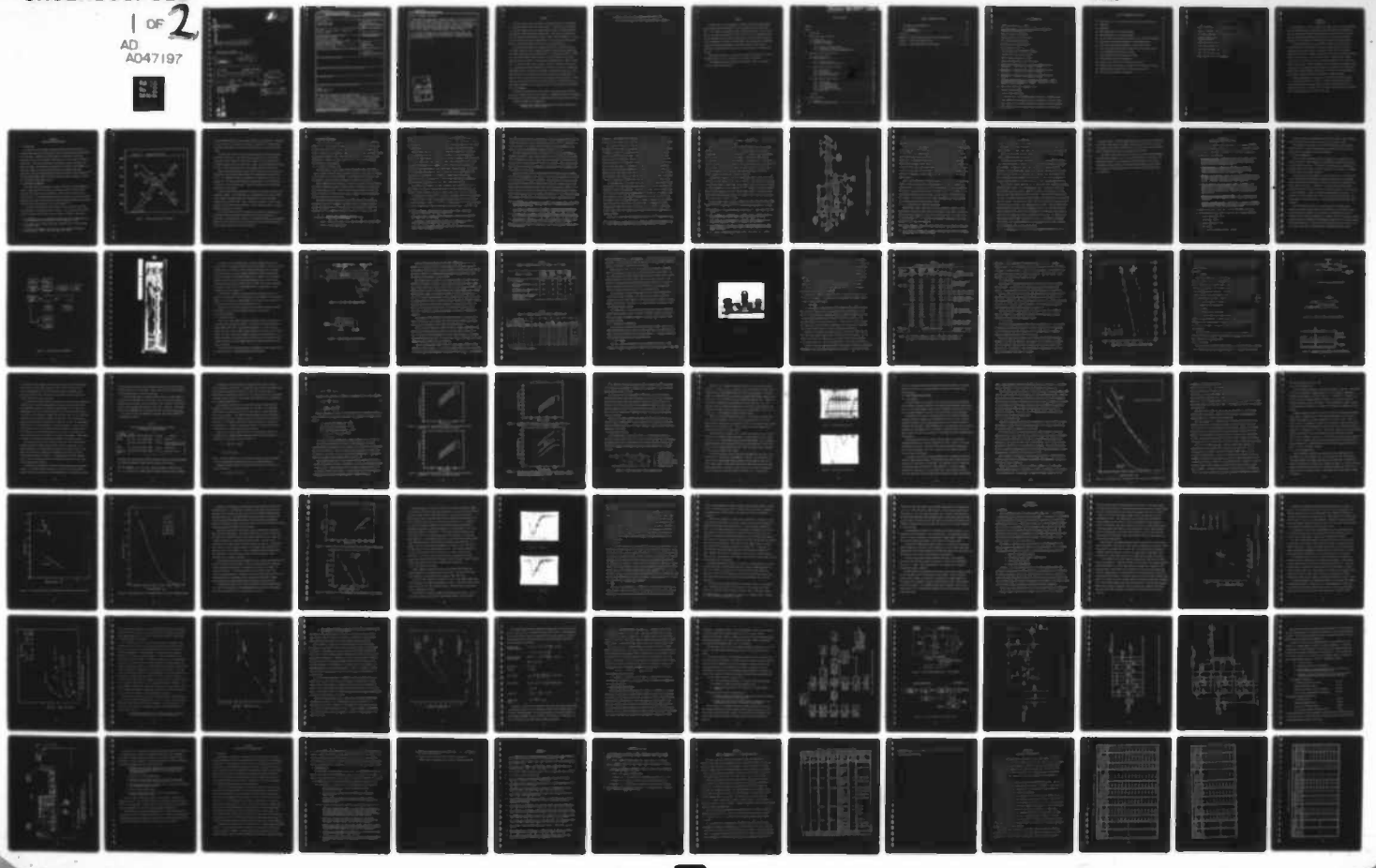

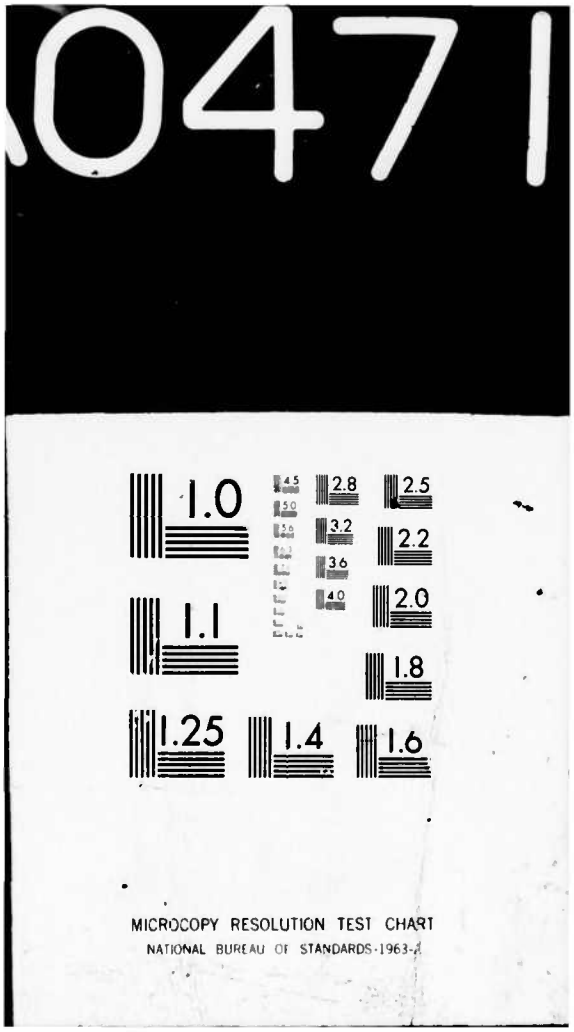
0471
1.0
1.1
1.25
1.4
1.6
1.8
2.0
2.2
2.5
2.8
3.2
3.6
4.0
4.5
5.0
MICROCOPY RESOLUTION TEST CHART
NATIONAL BUREAU OF STANDARDS-1963-A

(12) B.S

(15) N00014-76-C-0975

(6) LOW REPETITION RATE COPPER VAPOR LASER.

General Electric Company
Philadelphia, Pennsylvania 19101

(11) SEP[redacted]977

(13) 1PP.

(9) Final Report. JUN[redacted]976—MAY [redacted]977,

(10) Robert S. Anderson,
Robert J. Homsey
Thomas W. Karras

PHYSICAL SCIENCES DIVISION
OFFICE OF NAVAL RESEARCH
800 NORTH QUINCY STREET
ARLINGTON, VA. 22217

405 025

mt

UNCLASSIFIED

SECURITY CLASSIFICATION OF THIS PAGE *(When Data Entered)*

REPORT DOCUMENTATION PAGE		READ INSTRUCTIONS BEFORE COMPLETING FORM
1. REPORT NUMBER N00014-76-C-0975	2. GOVT ACCESSION NO.	3. RECIPIENT'S CATALOG NUMBER
4. TITLE *(and Subtitle)* LOW REPETITION RATE COPPER VAPOR LASER		5. TYPE OF REPORT & PERIOD COVERED Final Report June 1976 to May 1977
		6. PERFORMING ORG. REPORT NUMBER NONE
7. AUTHOR(s) Robert S. Anderson, Robert J. Homsey, and Thomas W. Karras		8. CONTRACT OR GRANT NUMBER(s) N00014-76-C-0975 NLW
9. PERFORMING ORGANIZATION NAME AND ADDRESS General Electric Company Space Sciences Laboratory P.O. Box 8555, Philadelphia, Pa. 19101		10. PROGRAM ELEMENT, PROJECT, TASK AREA & WORK UNIT NUMBERS
11. CONTROLLING OFFICE NAME AND ADDRESS Physical Sciences Div. - ONR 800 North Quincy Street, Arlington, Va. 22217 Attn: Dr. W. J. Condell		12. REPORT DATE May 1977
		13. NUMBER OF PAGES 101
14. MONITORING AGENCY NAME & ADDRESS*(if different from Controlling Office)*		15. SECURITY CLASS. *(of this report)* UNCLASSIFIED
		15a. DECLASSIFICATION/DOWNGRADING SCHEDULE

16. DISTRIBUTION STATEMENT *(of this Report)*

17. DISTRIBUTION STATEMENT *(of the abstract entered in Block 20, if different from Report)*

18. SUPPLEMENTARY NOTES

19. KEY WORDS *(Continue on reverse side if necessary and identify by block number)*

Lasers
Copper Vapor Laser
Visible Laser

20. ABSTRACT *(Continue on reverse side if necessary and identify by block number)*

This report describes the development and demonstration of a low repetition rate, discharge heated copper vapor laser (DHCVL). The purpose of the program is to develop a DHCVL with output characteristics capable of satisfying present Navy underwater communication and ranging needs. To achieve the program goals, tasks were undertaken encompassing a range of effort from the assembly of a laser test and evaluation facility to demonstration of a low PRF laser and conceptual design of a brassboard system suitable for Navy field applications.

DD FORM 1 JAN 73 1473 EDITION OF 1 NOV 65 IS OBSOLETE

UNCLASSIFIED

SECURITY CLASSIFICATION OF THIS PAGE *(When Data Entered)*

Block 20 - ABSTRACT (continued)

The program has resulted in a significant advance in the state-of-the-art. A laser module was demonstrated at a PRF of 1.0 kHz with a 12.12 mJ per pulse output, which is a factor of 7 greater than the prior art. The laser was operated consistently at a PRF as low as 700 Hz. Analysis of experimental data for a range of tube diameters and PRF values show that output pulse energy scales linearly with the active lasing volume. Significantly, no physical limit to this volumetric scaling was observed during the program.

It has been concluded that a laser system for producing greater than 50 mJ per pulse is feasible using two laser modules. A brassboard design can be assembled with moderate risk using electronic components within the present state-of-the-art.

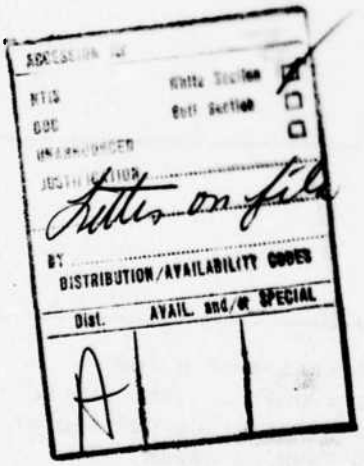

SUMMARY

This report describes the development and demonstration of a low repetition rate, discharge heated copper vapor laser (DHCVL). The purpose of the program is to develop a DHCVL with output characteristics capable of satisfying present Navy underwater communication and ranging needs. To achieve the program goals, tasks were undertaken encompassing a range of effort from the assembly of a laser test and evaluation facility to demonstration of a low PRF laser and conceptual design of a brassboard system suitable for Navy field applications.

The program has resulted in a significant advance in the state-of-the-art. A brassboard design has been established capable of satisfying the program goals for a DHCVL system with the characteristics of: >50 mJ per pulse output at 5105Å; <50 ns pulse width FWHM; overall efficiency >0.5%; PRF >500 Hz; and lifetime without refilling >10 hours. A laser module was demonstrated at a PRF of 1.0 kHz with a 12.12 mJ per pulse output, which is a factor of 7 greater than the prior art. The laser was operated consistently at a PRF as low as 700 Hz. Analysis of experimental data for a range of tube diameters and PRF values shows that output pulse energy scales linearly with the active lasing volume. Significantly, no physical limit to this volumetric scaling was observed during the program. Demonstration of a scaled up 25 mJ per pulse laser module was not possible because of the untimely availability of a larger test facility found necessary and assembled late in the program.

It has been concluded that a laser system for producing greater than 50 mJ per pulse is feasible using two laser modules. A brassboard design can be assembled with moderate risk using electronic components within the present state-of-the-art.

Further development is recommended to:

a) generate data to quantitatively extend the scaling parameters and determine their physical limits;

b) produce a 50 mJ per pulse brassboard laser system; and

c) field test and evaluate the laser system performance capabilities.

PREFACE

The major effort of this program is to extend the prior art for discharge heated copper vapor lasers (DHCVL) into the low repetition rate regime (500 < PRF < 2.5 kHz) while increasing the output pulse energy and power. The achievement of the program goals requires a proper balance to be made among many interrelated phenomena such as electrical discharge in low pressure gases, tube and copper temperatures, radiation shielding design, and pulse generation parameters. The extensive technical experience at the General Electric Space Sciences Laboratory on DHCVL development provides an excellent basis for achieving this balance.

Many people contributed to the successful completion of this work. Special thanks are given to Dr. B. G. Bricks, B. P. Fox and L. W. Springer.

The valuable discussions, suggestions and support of Dr. C. E. Anderson are also gratefully acknowledged.

TABLE OF CONTENTS

TABLE OF CONTENTS (Continued)

LIST OF ILLUSTRATIONS

LIST OF ILLUSTRATIONS (Continued)

LIST OF TABLES

SECTION I
INTRODUCTION

The development of discharge heated copper vapor lasers is proceeding steadily forward in both performance capabilities and satisfaction of user requirements. During the past fifteen months, the DHCVL has not only improved its output pulse energy, average power and peak power, but more than a dozen lasers have been delivered to the government for laboratory R&D activities and field operation.

The technology associated with the DHCVL is common to a broader class of lasers relying on the generation and excitation of metal vapors by electrical discharges in low pressure gases. The inherent design features of discharge heated metal vapor lasers (DHMVL) are providing a basis for a continually expanding sphere of application as they become better known to potential users. DHMVL features such as wavelength selection, performance flexibility (e.g., PRF, pulse widths, power output), inherent ruggedness, ease of maintenance, acceptable weights and volumes, and comparatively low investment and operating costs are supporting applications including airborne illumination for visible and near-IR sensors, dye laser pumps, isotopic separation and atmospheric propagation studies.

The present program is an entry into another potential application area, i.e., optical communication and ranging. The primary technological interests are the achievement of high peak powers and pulse energies at moderately low pulse repetition rates. Success with these issues would provide the technological base for advanced systems of interest to the Navy.

SECTION II
COPPER VAPOR LASER BACKGROUND

2.1 INTRODUCTION

For several years, development programs have been conducted with a goal of producing high efficiency lasers operating in the visible and near-visible portions of the spectrum. Currently, particular emphasis is being placed upon these systems with lines in the blue-green region because of a wide variety of possible applications. Among these applications are problems involving underwater transmission of light. The copper vapor laser which has a dominant line (5105Å) in the appropriate region of the spectrum is particularly promising because high efficiency and specific energy have been achieved in systems of small dimensions.[1,2] The high pulse energies needed for useful underwater detection ranges are expected to be reachable through modest scaling.

2.2 PRINCIPLES OF OPERATION

The copper vapor laser belongs to a family of efficient, pulsed-discharge gas lasers. Laser operation in this group is inherently pulsed or self-terminated because the lower laser state is metastable. Thus the basic processes have a cyclic pattern. A fast discharge pulse produces an inversion, and this is followed sequentially by laser oscillation and an extended period during which the metastable lower state must relax before the cycle can be repeated.[3]

The nature of this operation can be easily seen by referring to the energy level diagram of the copper atom shown in Figure 1. The upper laser states (4^2P) are excited from the ground state by direct electron collisions. These levels

---

1. R. S. Anderson, et al, "Discharge-Heated Copper Vapor Laser, MOPA Operation," Final Report AFAL-TR-76-93, Air Force Avionics Laboratory, (1976).

2. B. G. Bricks, et al, "Copper Vapor Laser," AFWL-TR-75-197, Air Force Weapons Laboratory, (1975).

3. W. T. Walter, N. Solimene, M. Piltch and G. Gould, "Efficient Pulsed Gas Discharge Lasers," IEEE J. Quan. Elec. QE-2, 474, (1966).

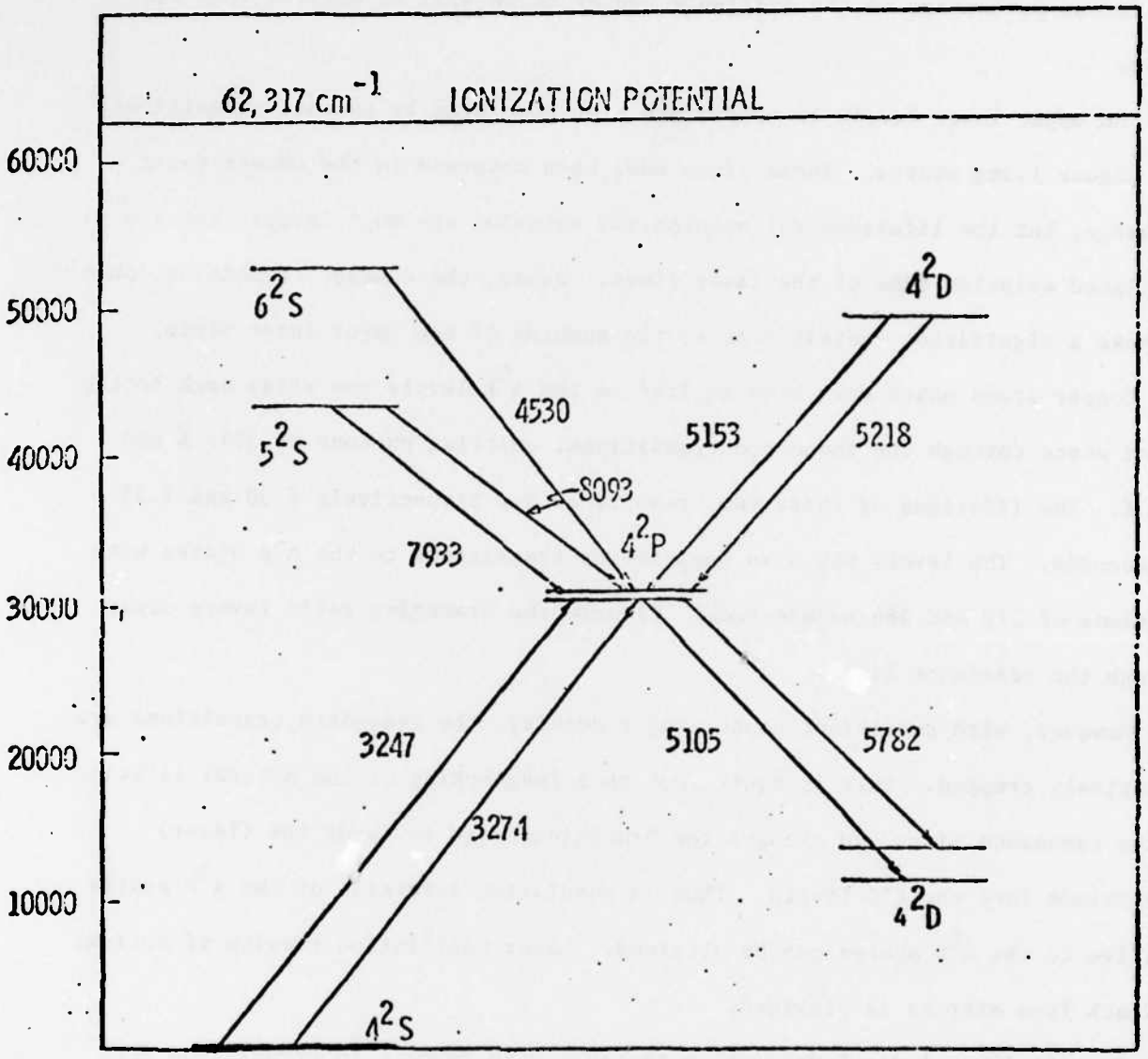

Figure 1. Copper Atom Energy Level Diagram

are the resonant states which are strongly coupled to the ground state. Therefore, the cross section for collisional excitation is large, and it is expected that a significant percentage of the available copper atoms will be excited into these levels.

The upper laser levels in copper are also populated by cascade transitions from higher lying states. These lines have been observed in the copper vapor discharge, but the lifetimes for spontaneous emission are much longer than the stimulated emission time of the laser lines. Hence, the cascade transitions should not make a significant contribution to the pumping of the upper laser state.

Copper atoms which have been excited to the 4^2P levels can relax back to the ground state through the resonance transitions, emitting photons of 3247 Å and 3274 Å. The lifetimes of these two transitions are respectively 7.30 and 7.35 nanoseconds. The levels may also deexcite by transitions to the 4^2D states with lifetimes of 512 and 485 nanoseconds. Clearly the branching ratio favors decay through the resonance lines.

However, with sufficient copper vapor density, the resonance transitions are radiatively trapped. This is equivalent to a lengthening of the natural lifetime of the resonance lines and changes the branching ratio to favor the (laser) transitions into the 4^2D levels. Thus, a population inversion of the 4^2P states relative to the 4^2D states can be obtained. Laser oscillation results if optical feedback from mirrors is provided.

The 4^2D lower laser levels are metastable with respect to transitions into the ground state because quantum mechanical selection rules prohibit $\Delta\ell = 2$ transitions. Laser oscillation, therefore, is necessarily pulsed or self-terminated because the lower levels must relax by relatively slow collisional processes with other discharge constituents or walls of the tube.

2.3 HISTORICAL DEVELOPMENT

Laser oscillation in atomic copper vapor was first reported in 1966[3] by Walter et al. In this paper the results of the first experiments with a copper system were described, and a general discussion of the basic concepts of this class of pulsed laser was presented. Many possible laser lines in several different elements were identified, and in the intervening time period several have been demonstrated. However, of these, copper still has shown the most promising characteristics and development.

2.3.1 Production of Copper Vapor

The production of a copper vapor density sufficiently high ($\sim 10^{14}/cm^3$) to trap the resonance line and produce population inversion requires that the copper metal be heated to at least 1400-1500°C. This requirement has resulted in the development of several different techniques for producing copper vapor.

These temperatures were achieved in the first copper vapor laser by placing the alumina discharge tube which contained pieces of copper and an appropriate buffer gas inside an oven.[3] The oven was electrically heated, and, when the proper discharge tube temperature was reached, a pulsed electrical discharge was applied, producing laser oscillation.

Experiments performed with the oven-type laser have produced significant performance results and fundamental information about the atomic processes of the system. For example, Walter[4] has reported a 1.2% discharge efficiency* and, more recently[5] has achieved an average output power of 11 watts, one of the

---

*Discharge Eff = $\frac{\text{Energy Stored on Discharge Capacitor}}{\text{Energy Output in Laser Pulse}} \times 100$

4. W. T. Walter, "40kW Pulsed Copper Laser," Bull. Am. Phys. Soc. 12, 90 (1967).

5. W. T. Walter, private communication.

higher values reported. While in the same laboratory, Chimenti[6] performed a detailed investigation of the fundamental properties of the copper laser. Included among the measurements were a parametric study of the output properties, the relaxation mechanisms of the lower laser states, line shapes, and single-pass gain.

Despite these impressive results, the oven-heated copper laser has several serious drawbacks which severely limit its prospects as a practical system for applications. Most important is the electrical energy consumed by the heater units in the oven. This power input exceeds all other power requirements of the laser and makes the attainment of an overall efficient system virtually impossible. Furthermore, the oven technique creates additional thermal problems. All elements of the laser head (including the oven) are subjected to very high temperatures increasing the vulnerability of the system to thermal shocks and stresses. In addition, the entire system has such a large thermal mass that the attainment of stable operating temperatures and laser output takes several hours.

The obvious shortcoming of the high temperature oven technique has led to the development of a variety of alternative methods of copper vapor production. For instance, several different sources of flowing copper vapor have been developed.

An exploding wire plasma gun[7] was used to investigate laser pulse lengthening by having a continual supply of copper atoms flowing into the active zone during the excitation pulse. Russell et al.[8] have obtained laser action with arc heating and nozzle expansion as a means of producing the flowing copper. Ferrar[9] inves-

---

6. R. J. L. Chimenti, "The Copper Vapor Laser," Ph.D. Thesis, Polytechnic Institute of Brooklyn, June 1972. (unpublished)

7. J. F. Asmus and N. K. Moncur, "Pulse Broadening in a MHD Copper Vapor Laser," App. Phys. Lett. 13, 384 (1968).

8. G. R. Russell, N. M. Nerheim and T. R. Pivirotto, "Supersonic Electrical-Discharge Copper Vapor Laser," App. Phys. Lett. 21, 565 (1972).

9. C. M. Ferrar, "Copper-Vapor Laser with Closed-Cycle Transverse Vapor Flow," IEEE J. Quan. Elec. QE-9, 856 (1973).

tigated a boiler system for the same purpose. Finally, a surface-tension-limited copper vapor generator has been developed by Karras et al.[10] A parametric study of the properties of a flowing copper vapor laser using this generator as the source of copper was subsequently reported by Bricks et al.[2]*

The high temperatures which were required in all the above experiments to produce the density of copper vapor needed for laser oscillation led to a search for low temperature sources of copper. The most successful of these efforts has been the use of copper halides[11-13] (CuCℓ, CuI or CuBr). These compounds have the required vapor pressure at temperatures significantly lower (400-800°C) than those needed for pure copper.

During early experiments the salts were vaporized by placing the discharge tube into a low-temperature oven. Lasers of this type were operated in a double-[11] or multiple-pulse[12,13] mode of operation. In the former case, the first pulse dissociated the molecular vapor producing free copper and halogen atoms. If the second pulse was appropriately timed, laser oscillation could be produced. In the latter case, the first pulse of the train was a pure dissociating pulse whereas each succeeding pulse caused both lasing and dissociation. Thus, a balance between recombination and dissociation was established leading to continuously pulsed

10. T. W. Karras, R. S. Anderson, B. G. Bricks, T. E. Buczacki and L. W. Springer, "Copper Vapor Generator," AFWL-TR-73-133, Air Force Weapons Laboratory, Kirtland AFB, NM (1973).

11. C. J. Chen, N. M. Nerheim and G. R. Russell, "Double-Discharge Copper Vapor Laser with Copper Chloride as a Lasant," App. Phys. Lett. 23, 514 (1973).

12. C. J. Chen and G. R. Russell, "High-Efficiency Multiply Pulsed Copper Vapor Laser Utilizing Copper Chloride as a Lasant," App. Phys. Lett. 26, 504 (1975).

13. I. Liberman, R. V. Babcock, C. S. Liu, T. V. George and L. A. Weaver, "High-Repetition-Rate Copper Iodide Laser," App. Phys. Lett. 25, 334 (1974).

*The results of the parametric study will be referred to throughout when necessary to the discussion.

operation. Unfortunately, this balance may be practically achievable only at high rates (e.g., greater than 10 kHz) thus limiting the usefulness of the system.

The ultimate efficiency of this type of system could be reduced over that obtainable in a pure metal device because each molecular dissociation requires an expenditure of energy to release the halogen atoms. At high repetition rates, where the interpulse period is short compared to the recombination time, this energy loss will be minimized. However, the presence of large quantities of the halogen atoms will, of course, still provide a potential source of energy loss in the electrical discharge. Furthermore, the lower discharge tube temperature, which on the one hand appears beneficial for obvious reasons, is a serious disadvantage where high average power must be rejected as waste heat. This situation will inevitably occur because the rejected power will be on the order of kilowatts even for a one percent efficient laser operating at a few tens of watts output.

The discharge-heated pure copper vapor laser offers a technique which circumvents several of the above-mentioned disadvantages. The required discharge tube temperature (copper vapor density) is achieved by a proper balance of input power to the electrical discharge and thermal radiation shielding of the discharge tube. Thus, because the waste heat from the discharge which excites the copper atoms also heats the tube, no additional source of energy is required, and the overall system efficiency of this laser is very high ($\sim$1%). In addition the 1400^{o}C discharge tube temperature allows the simple radiative rejection of waste heat. Finally, copper atoms are available at all times permitting the widest range of repetition rates.

This type of laser was first reported by Isaev et al.[14] Subsequent demon-

14. A. A. Isaev, M. A. Kazaryan and G. G. Petrash, "Effective Pulsed Copper-Vapor Laser with High Average Power Generation," JETP Lett. 16, 27 (1972).

strations have been reported in this country by Fahlen[15] and Anderson et al.[16]

2.3.2 Electrical Discharge Techniques

The copper vapor laser is pumped by high repetition rate, narrow current pulses. The current pulse widths have in the past ranged from a maximum of approximately 1 μsec[3] to as low as 10 nsec.[2] In general, most experiments have been performed with pulses in the range of 400-100 nsec FWHM, though narrower pulses have been continually sought in this laboratory by reduction of circuit inductance. This is expected to improve the efficiency of the laser because the rise time of the current is reduced, the peak current is increased and less energy is deposited in the discharge tube after laser pulse termination. A typical component configuration is shown in Figure 2.

Typical pulse repetition rates for the discharge-heated laser were, before the start of this program, in the range of 3-20 kHz. Operation below this range had only been common in lasers which do not require discharge heating to maintain the tube temperature and vapor density.[3,8,9,18] However, the General Electric Space Sciences Laboratory in early 1976 had begun an effort to develop a high pulse energy discharge-heated copper vapor (DHCVL) laser with pulse repetition rate in the range of 200 Hz to 2 kHz.

The switching of these high rate discharges has been done with either spark gaps[2,9,10,19] or thyratrons.[1-3,16] The thyratrons have proven to be more

15. T. S. Fahlen, "Hollow-Cathode Copper-Vapor Laser," J. Appl. Phys. 45, 4132 (1974).

16. R. S. Anderson, L. W. Springer, B. G. Bricks and T. W. Karras, "A Discharge-Heated Copper Vapor Laser," IEEE J. Quan. Elec. QE-11, 173 (1975).

17. A. A. Isaev, M. A. Kazaryan and G. G. Petrash, "Copper Vapor Laser with a Repetition Frequency of 10kHz," Opt. Spectros. 35, 307 (1973).

18. L. A. Weaver, C. S. Liu and E. W. Sucov, "Superradiant Emission at 5106, 5700 and 5782 Å in Pulsed Copper Iodide Discharges," IEEE J. Quan. Elec. QE-10, 140 (1974).

19. W. E. Austin, "100kHz Quenching Spark Gaps," Laser Focus 11, 79 (1975).

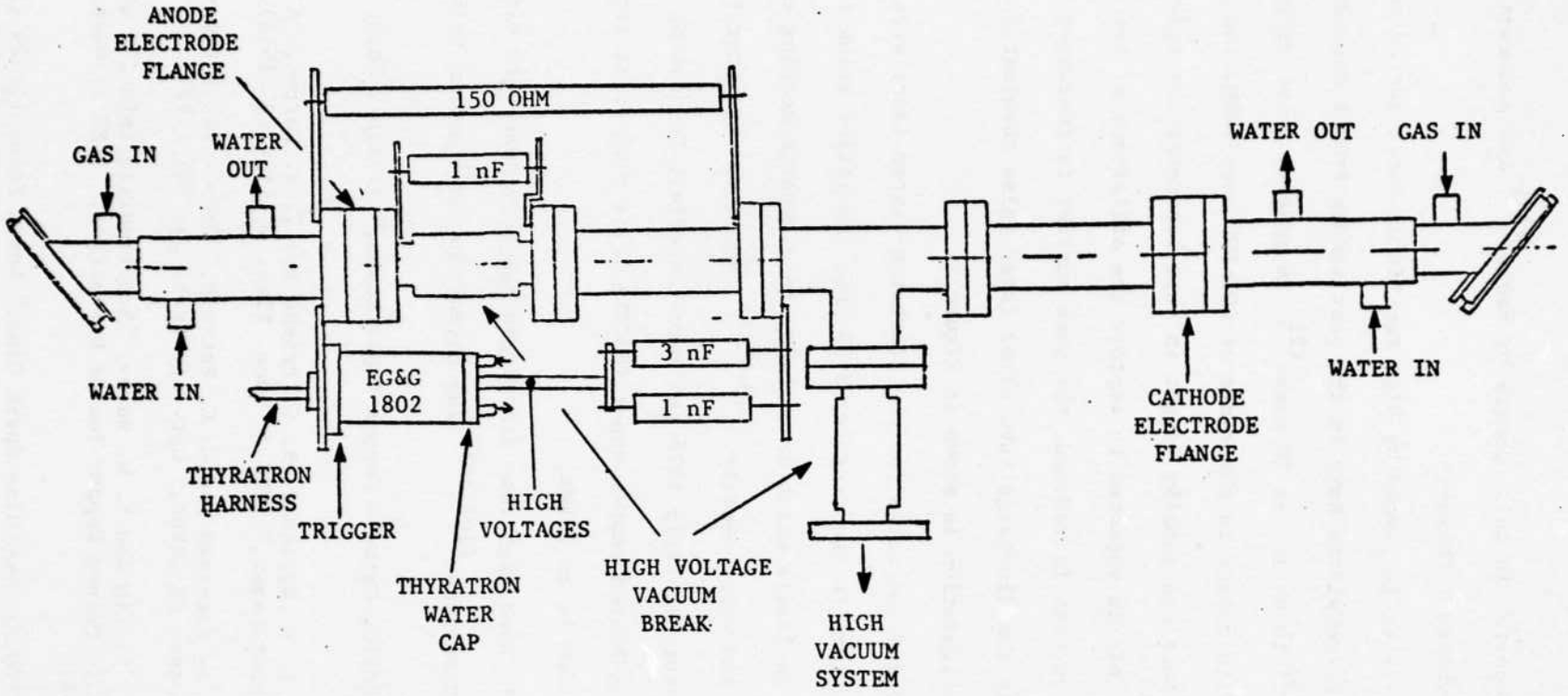

Figure 2. Schematic Diagram of the Laser Head Showing the Components of the Pulsed Electrical Discharge Circuit

practical devices for long term, steady state operation because of their long lifetime characteristics when switching average powers in the range of 1-2 kW.

Laser oscillation has been achieved with both longitudinal discharges parallel to the laser axis[6,10,14,16,18] and transverse discharges perpendicular to it.[2,10,15,20] The latter category includes hollow cathode devices[15,20] in which the discharge takes place between a slotted cathode tube and an enclosing anode tube. A principal difference between the longitudinal and transverse discharges is the peak current required to produce a specific output energy. The latter has led to very high current density and high specific energy output but at a cost of a very small active volume.[9] Only the longitudinal discharge seems capable of scalability to large volumes with high current density and limited peak currents.

Such a laser system can be scaled in volume by simultaneously increasing tube diameter, length and peak current while maintaining the specific energy at an adequate level. For instance, 50 $\mu J/cm^3$, as demonstrated in early experiments, could lead to a pulse energy of 50 mJ if produced in the active volume of a 1.5 inch diameter discharge tube 90 cm long. A peak current of 5,000 amps should be required. It is important to note though, that significant pulse energies can be reached with much lower specific energy.

2.3.3 Low Repetition Rate Discharge Techniques

Historically, copper vapor lasers have been operated at repetition rates greater than 5 kHz and very little has been reported at lower rates. William T. Walter has reported operating a 0.6 watt average power laser at 1.5 kHz in an oven-heated device.[21] His laser was very efficient, converting 1.77% of the discharge energy into laser output.

---

20. R. S. L. Chimenti, "Heat-Pipe Copper Vapor Laser," Final Report to Contract N0014-73-C-0317, 1974.

21. W. T. Walter, Polytechnical Institute of New York, Joint Services Technology Advisory Report No. R452-41-76 (1976).

Up to 11 mJ/pulse on a single shot basis has been obtained at JPL[22] but they do not report any operation in the repetition rate range between 0.5 and 1.0 kHz.

Alexandrov[23] reports the operation of a transverse discharge copper vapor laser operating at 1.0 kHz. His output power is 0.1 watts which is relatively low.

Thus very little data has been reported in the open literature or through personal communication about operation at low rates.

Before this contract began, the GE-SSL had operated discharge-heated copper vapor lasers at repetition rates as low as 1.8 kHz where approximately 2 mJ/pulse were obtained. At repetition rates below this, several problems occurred. Primarily, the discharge became unstable since the peak currents in the thyratron and the peak voltages on the capacitors were exceeding their specifications and stray discharges occurred within the vacuum jackets. Still only a minimal effort had been made to reduce this repetition rate and so the problems remained unsolved.

Even with this limited experience at low repetition rates, several encouraging observations were noted. First the energy/pulse was continuing to increase as the repetition rate was lowered. There was no sign of any leveling off to some specific pulse energy which could not be exceeded. Secondly, the lasers were able to operate at higher temperatures and hence higher copper densities as the repetition rate was reduced. This means more copper atoms were available for lasing and hence a higher theoretical limit to any maximum energy per pulse. The third significant observation was the increase in the breakdown voltage of the discharge tube with lower repetition rates. This was due presumably to the decrease in ions and free electrons in the plasma just prior to initiation of the pulse. The longer inter-pulse period permitted more recombination to occur. The increase in breakdown voltage meant that the main capacitor in the discharge circuit could be charged

22. G. R. Russell, JPL, private communication.

23. I. S. Alexandrov, et al, Soviet Journal of Quantum Electronics, Vol. 5, No. 9.

to a higher voltage. With this increase voltage, the average power needed could be put into the discharge tube without increasing the main capacitor and hence the discharge pulse length. This applied up to the rated value of the capacitor which as stated earlier limited use to greater than 1.8 kHz.

The present program has built on this data base to explore and demonstrate increased pulse energies and lower pulse repetition rates. The results, to be discussed in detail in later sections, clearly demonstrate a factor of six improvement in pulse energies (12 mJ/pulse) and the potential for even higher pulse energies as the input energy per unit volume and active volume itself are increased.

SECTION III

DEVELOPMENT APPROACHES AND RESULTS

The technical effort followed during the course of the program was grouped into several tasks whose general objective was to explore and demonstrate different facets of low repetition rate DHCVL performance that would lead to improved output characteristics. The tasks were:

- Facility Construction - implementation of a test facility capable of handling discharge tubes of up to 1-3/4" ID, suitable for Master Oscillator Power Amplifier (MOPA) operation, and having suitable diagnostic measurement capability.

- Switch Evaluation - experimental evaluation of a variety of commercially available thyratrons and techniques for use in producing high peak currents ($\sim 10^4$ amps) and fast rise times ($\sim$50 ns) discharge pulses at low repetition rates.

- Design of Low Rate Laser - design, operation and evaluation of a low PRF DHCVL with proper radiation shield design, high current densities and basic diagnostic measurements including pulse energy, discharge voltage and current, tube temperature, pulse shapes, etc.

- Test and Evaluation of Large Diameter Tubes - experimental test and evaluation of different diameter laser tubes leading to a demonstration of a laser module design with an output of 25 mJ per pulse, using tube diameters of at least 1½" ID and adequate current densities as controlled by circuit elements, voltage and switch characteristics.

- Master Oscillator Power Amplifier (MOPA) - test, demonstration and evaluation of a MOPA configuration with an output pulse energy of 50 mJ/pulse.

- Conceptual Brassboard Design - generation of a conceptual brassboard design suitable for Navy field applications and based on operational characteristics of the laboratory breadboard DHCVL.

The overall program goal toward which the above individual efforts are directed is the demonstration of a DHCVL device with the following parameters:

- output energy/pulse > 50 mJ
- pulse width < 20 ns
- overall efficiency > 0.5%
- PRF > 200 Hz
- tube lifetime without refilling > 10 hours

The body of this section provides details on the technical effort conducted during the program and the results achieved in each of the six tasks.

The importance of scalability of the laboratory DHCVL to pulse energies greater than 50 mJ is sufficiently great that a separate section (4.0) on the subject has been included for clarity and emphasis.

3.1 FACILITY CONSTRUCTION

The first task accomplished during this program was the assembly of the laser test facility. This included the vacuum system, the laser vacuum envelope and the electronic circuitry. In addition a gas handling system consisting of a pressure gauge and flow control valves was attached to the facility. A schematic for the facility is provided in Figure 3.

For the majority of the program a vacuum envelope with a 2-3/8" ID was used. It was constructed from Varian Vacuum components called Nipples (Varian Model Number 952-5034) which were straight sections of stainless steel tubing 8¼" long with flanges on both ends. In addition, a Tee section (Varian Model Number 952-5037) was used to connect the envelope to the vacuum system. The last section of this envelope was a ceramic voltage break manufactured by Ceradyne Inc. It consists of a 2½" OD alumina tube 3" long with nickel brazed on each end. The total length of this section is 4.75". Figure 4 shows the vacuum envelope fully assembled.

This size envelope proved to be too small for 1½" ID discharge tubes because not enough radiation shield could consistently be fit between the laser tube and the vacuum envelope. This meant that the discharge tube could not consistently reach operating temperatures. Toward the end of the program, a second envelope facility was assembled using components manufactured by the Space Sciences Laboratory machine shop. It had an ID of 3¼" and was 44" long total length. The 1½" ID laser tube plus its radiation shield fit inside with room to spare.

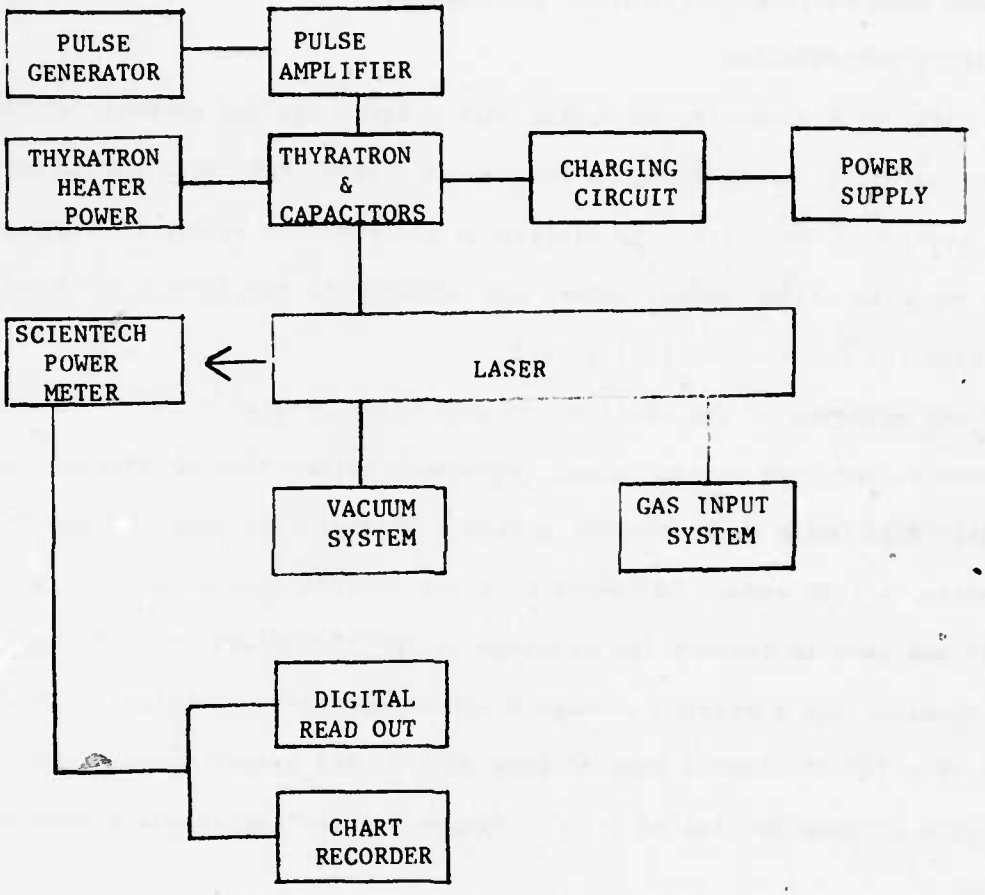

Figure 3. Laser Test Facility Components

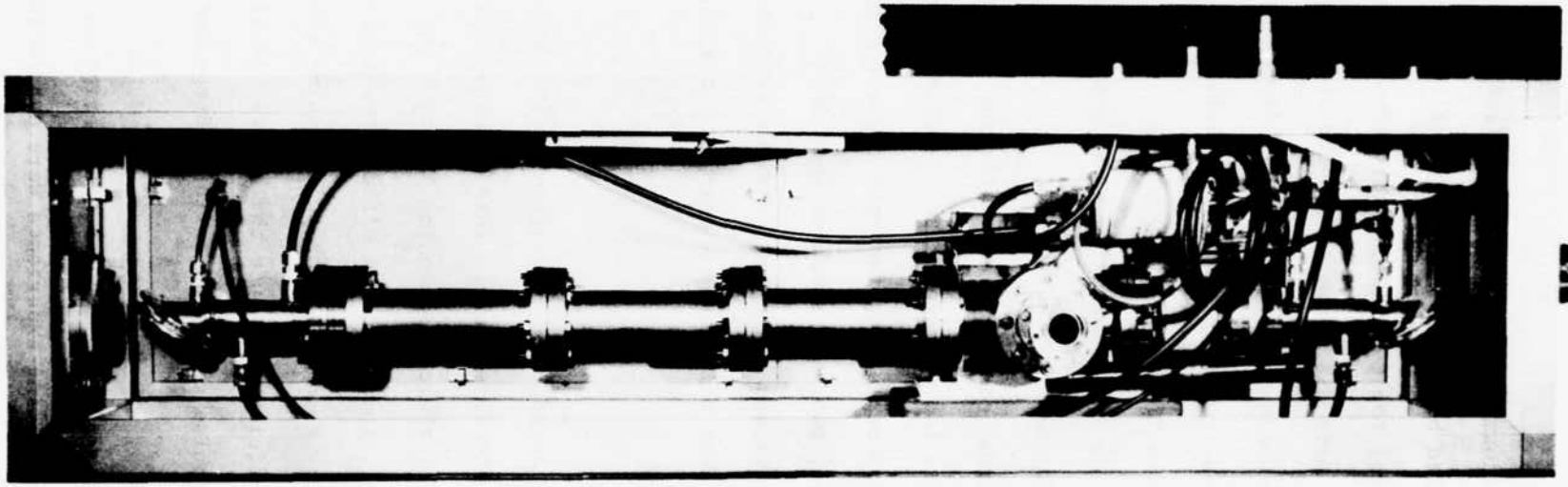

Figure 4. Discharge Heated Copper Vapor Laser

In addition to the vacuum envelope, all the electronic components and circuits had to be assembled before the facility was complete. These parts can be divided into two categories; the main discharge components and the thyratron triggering circuits. The main discharge components included energy storage capacitors purchased from Condenser Products Inc., inductors for the resonant charging circuits purchased from Capacitor Specialists Inc., and thyratrons purchased from IT&T, English Electric Valve, and EG&G. All of these components were mounted on the laser or in individual boxes. A block diagram of their arrangement is shown in Figure 3.

The thyratron triggering circuits were different for each thyratron. In general they consisted of a low voltage pulse, a pulse amplifier and a grid bias supply. Each of these are coupled together and connected to the thyratron. For the double grid thyratrons, two bias supplies were used.

After the test facility was assembled, various size laser tubes were built and operated. The results of this study appear in later sections.

3.2 SWITCH EVALUATION

3.2.1 Inductance Effects

The use of a pulse charged capacitor effectively reduces the inductance of the current path through the laser tube. This results in a higher di/dt and a smaller FWHM current pulse, thereby enhancing lasing. The use of the pulse charged capacitor, however, lowers system efficiency since energy is lost in the transfer of charge from the main capacitor to the pulse charged capacitor. It would be desirable to sufficiently reduce the entire circuit inductance so as to eliminate the need for a pulse charge capacitor. Steps were taken to try and achieve this goal.

The laser used for these tests was a 5 watt design as shown in Figure 5 and for which many hours of operating experience were available.

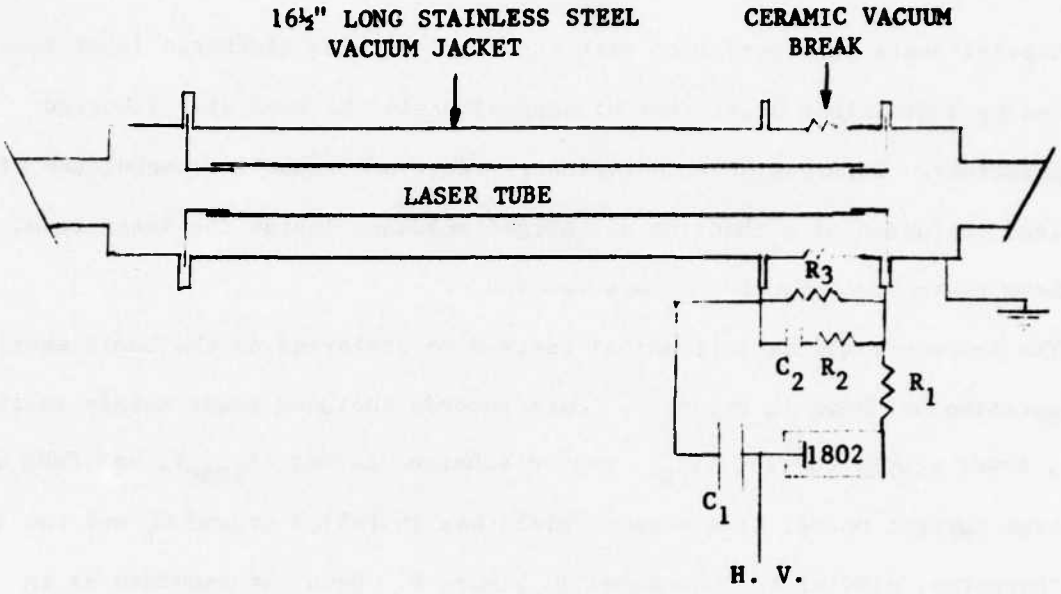

Figure 5. Test Laser and Charging Network

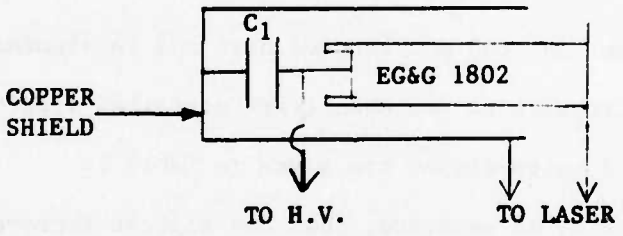

Figure 6. Shielded Capacitor and Thyratron

Initial tests were performed with the usual alumina discharge laser tube replaced by a stainless steel tube of approximately the same size (shorted configuration). This was done to evaluate inductance reduction techniques without the added confusion of a changing discharge impedance inside the laser tube. For these tests the capacitor C_2 was removed.

The procedure was as follows: a) tests were performed on the basic shorted configuration as shown in Figure 5. Data records included power supply voltage (E_{PS}), power supply current (I_{PS}), peak discharge current (I_{PEAK}), and FWHM of that discharge current pulse; b) a copper shield was installed around C_1 and the 1802 EG&G thyratron, similar to that shown in Figure 6. Data was recorded as in step a; c) a copper shield, similar to that around the 1802 and capacitor C_1 was installed around the ceramic vacuum break and data recorded; d) a metallic shield was placed inside the vacuum housing around the SS shorting tube. This was used as a low inductance current return. The results are given in Table 1. Obviously, a significant decrease in inductance with the use of shielding is indicated.

The stainless steel shorting rod was removed next and an alumina ceramic laser tube installed. The results of the same tests performed with the laser operating at approximately 5 watts output are given in Table 2.

The test results indicate, as expected, that the biggest improvements come with current pulse shortening and increase of the discharge current rate of rise. This can be done with addition of a pulse charge capacitor or shielding, the former being more effective. A current rate of rise of 10^{10} amp/sec and a width (FWHM) of 50-60 ns produce the best operation.

The use of shielding by itself without the pulse charged capacitor seems inadequate in most instances. It can be said, however, that the use of shielding does help efficiency when compared to a non-pulse charge circuit. In an unshielded

Table 1

Impact of Inductance Reduction Technique: Shorted Laser

Reduction Technique	Power Supply Voltage (volts)	Power Supply Current (mA)	Peak Current (A)	Pulse Width FWHM (10^{-9} sec)
a. No Shielding	500	195	294	108
b. Shielding on Capacitor C_1 and Thyratron	500	175	372	80.5
c. Shielding on C_1, Thyratron and Ceramic Vacuum Break	500	150	370	66.6
d. Shielding on C_1, Thyratron and Ceramic Break and Internal Current Return	500	135	372	58.3

Table 2

Impact of Inductance Reduction Technique: Operating Laser

Reduction Technique				Capacitor C_1 (nf)	dI/dt (10^9 A/sec)	Peak Current (A)	Pulse Width FWHM (10^{-9} sec)	Power Output (watts)	Laser Efficiency(2)	Efficiency Improvement
Shielding										
C_1 and Thyratron	Vacuum Break	Internal Return	Capacitor(1) C_2 Present							
		X		5	7.2	362	130.5	4.16	0.49	+21.7%
		X	X	5	10.2	612	60	5.01	0.59	
X	X	X		5	8.0	320	111	4.63	0.55	+7.2%
X	X	X	X	5	15.0	571	55.5	4.93	0.59	
		X		3	13.8	330	100	4.93	0.56	+8.9%
		X	X	3	32.6	489	54.4	5.1	0.61	
		X	X	5	24	489	60	4.8	0.55	Calibration Run
X	X	X		3	15.5	388	77	5.21	0.58	-1.9%
X	X	X	X	3	28	566	35.5	4.8	0.55	

Notes: (1) Capacitor C_2 = 1 nf

(2) Input power held constant for comparison

system the deletion of the pulse charged capacitor results in a 16.9% decrease in efficiency while in a shielded system the deletion of the pulse charge capacitor results in only about a 6% decrease in efficiency.

Reduction of C_1 from 5 nF to 3 nF also improved performance, presumably due to the increase in current rate of rise and decrease in pulse width. In fact, the most efficient laser operation in these tests resulted from an unshielded system, except for the current return, using a pulse charge capacitor. The addition of shielding decreased performance despite a high rate of current rise. This is believed to have resulted from the decrease in current pulse width (35 ns) to values too close to that of the laser pulse width.

The advantage of the pulse charge capacitor over just shielding could be due to the fact it delays breakdown of the laser tube long enough to allow the thyratron to go into full conduction. This allows maximum voltage to be impressed across the laser tube. Thyratron turn-on time may well be the limiting factor in a non-pulse charged system.

In summary then it can be said that the shielding technique shows promise but much work remains to be done. The pulse charging technique, in addition to being much easier to implement, produces at this time a more efficient laser in most situations.

3.2.2 Thyratron Tube Evaluations

Four different thyratrons were tested during this program. They were the 1802 and HY-5 manufactured by EG&G, the CX1174 manufactured by English Electric Valve, and the F-155 manufactured by IT&T (see Figure 7). The basic parameters and operating results of each are discussed below.

1. HY-5 (EG&G)

The first thyratron tested for low rate operation was the HY-5. This thyratron is rated at a peak anode voltage of 40 kV and a peak current of 5000 amps.

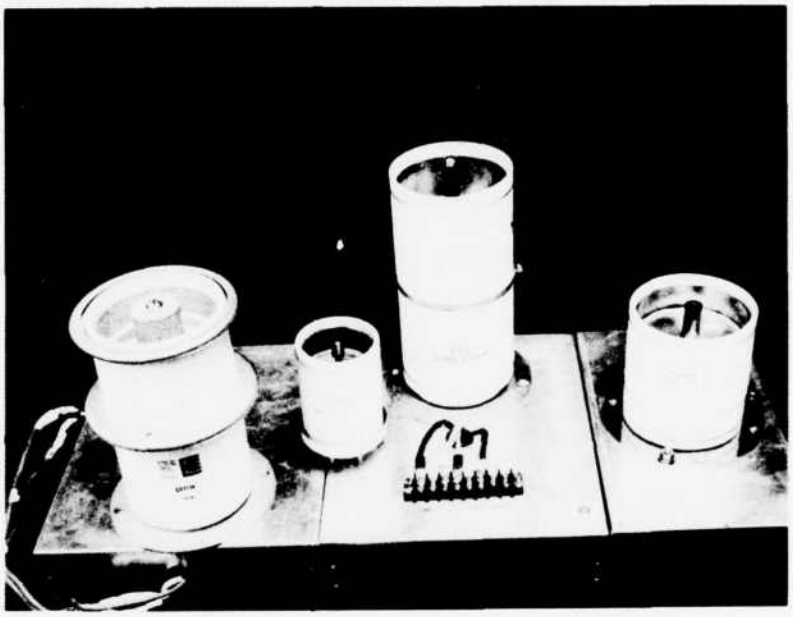

Figure 7. Four Thyratrons Tested

The particular thyratron tested in this experiment was calculated to require inductances greater than 1.0 henry in the resonant charging circuit to "shut off" during the interpulse period. Since high voltage inductors of this value were not available at that time resistive charging was turned to. Unfortunately, because half the input power must be dissipated in the charging resistors the lasers could not be run at even moderate powers with available power supplies.

Command charging, in which a second thyratron delays the application of voltage on the main thyratron for a time span sufficient to insure shut off could have been used but was not tried since the main scope of the program did not dictate major electronic circuit changes.

Consequently, because of these difficulties, no test data were accumulated with the HY-5 thyratron. It is possibly still a satisfactory switch, however, and may be worth further study.

2. 1802 (EG&G)

The second device evaluated was an 1802 hydrogen filled ceramic thyratron. This switch was being used in our high repetition rate experiments, but was limited to peak currents of 1500 amps. The main problem at higher currents was the poor anode dissipation which caused the electrode to glow red hot and eventually destroy the ceramic-metal seals. By application of water cooling to the anode plate, the peak current capabilities were extended to over 4000 amps and in select cases currents in excess of 5000 amps were possible.

Because of its design, this thyratron shut off much more quickly than the HY-5, and thus resonant charging with only 300 m henries was possible. For this reason it was used in the early work at low repetition rates and produced an 11.2 mJ/pulse laser at 1.2 kHz, as discussed later in this report (see Table 3).

The water cooling of the anode provided an easy means of making a calorimetric measurement of the power being deposited in the thyratron. This varied between

Table 3

Performance Comparison of Thyratron Switches[1]

Thyratron Unit	Input Power (watts)	Capacitor Ratio[2] (nf/nf)	Output Energy (mJ/Pulse)	Test Date	Comments
EG&G 1802	2190	25/6	11.15	Nov. 19, 1976	First high pulse energy output
	2000	25/6	8.09	Mar. 3, 1977	Laser output limited by heat shield effectiveness
	2194	25/6	8.74	Mar. 3, 1977	
EEV CX1174	1993	25/6	8.14	Mar. 8, 1977	
	2203	25/6	8.81	Mar. 11, 1977	
	2300	25/6	10.0	Mar. 29, 1977	New laser tube & improved heat shield effectiveness
	2369	25/6	10.2	Mar. 11, 1977	
	2200	20/6	10.8	Mar. 11, 1977	More effective energy coupling into laser with this capacitor ratio
	2388	20/6	11.15	Mar. 11, 1977	
ITT F-155	2337	20/6	10.18	Apr. 1, 1977	Thyratron permitted operation at higher input currents & power
	2360	20/6	10.15	Apr. 1, 1977	
	2379	20/6	10.73	Apr. 1, 1977	
	2081	20/6	10.0	Apr. 1, 1977	
	2532	20/6	10.97	Apr. 1, 1977	
	2750	20/6	11.2	Apr. 1, 19777	
	2400	20/9	11.45	Apr. 1, 1977	More effective energy coupling into laser with this capacitor ratio
	2654	20/9	11.9	Apr. 1, 1977	
	2925	20/9	12.12	Apr. 1, 1977	
EG&G HY-5	COULD NOT OPERATE LASER				Insufficient inductance available

Notes: (1) All lasers compared at a PRF = 1 kHz; laser tube lengths = 46"

(2) Ratio of energy storage capacitor to pulse charge capacitor

about 10% to 22% depending upon the input power and the length of the laser. Figure 8, based on data in Appendix C, gives the thyratron dissipation for typical conditions. No clear patterns of behavior that would indicate what variable could be changed to minimize this loss further was apparent. This may thus be a loss inherent to the thyratron that cannot be avoided.

3. CX1174 (EEV)

This switch is a deuterium filled ceramic thyratron manufactured by English Electric Valve. It is rated at 40 kV peak anode voltage and 6000 amps peak current. It specifications are ideal for this low repetition rate application.

When this thyratron was first tested, the same problems that plagued the HY-5 reoccurred. Fortunately, over 2 henries of inductance were now available for the resonant charging circuit and satisfactory operation at low repetition rates was obtained. At 1.0 kHz, the laser's performance with an EG&G 1802 thyratron and with an EEV CX1174 thyratron were similar (see Table 3).

The thyratron did, however, operate at repetition rates as low as 600 Hz where the 1802 would not. This clear advantage for the CX1174 thyratron was surpassed by the next and last thyratron tested.

4. F-155 (ITT)

An F-155 thyratron, manufactured by IT&T, is a modified F-117. It is capable of operating at a peak anode voltage of 33 kV and a peak current of 10,000 amps. It can also operate the 6 kHz repetition rates and higher which, of course, implies no problem in shutting off at lower rates.

When this thyratron was connected to the laser, the performance was also identical to the 1802 at comparable input powers. It did, however, run reliably with up to 40% more input power which ultimately led to the 12 mJ/pulse laser (see Table 3). In addition, it operated steadily at repetition rates as low as 600 pps with minimal "shutting off" problems.

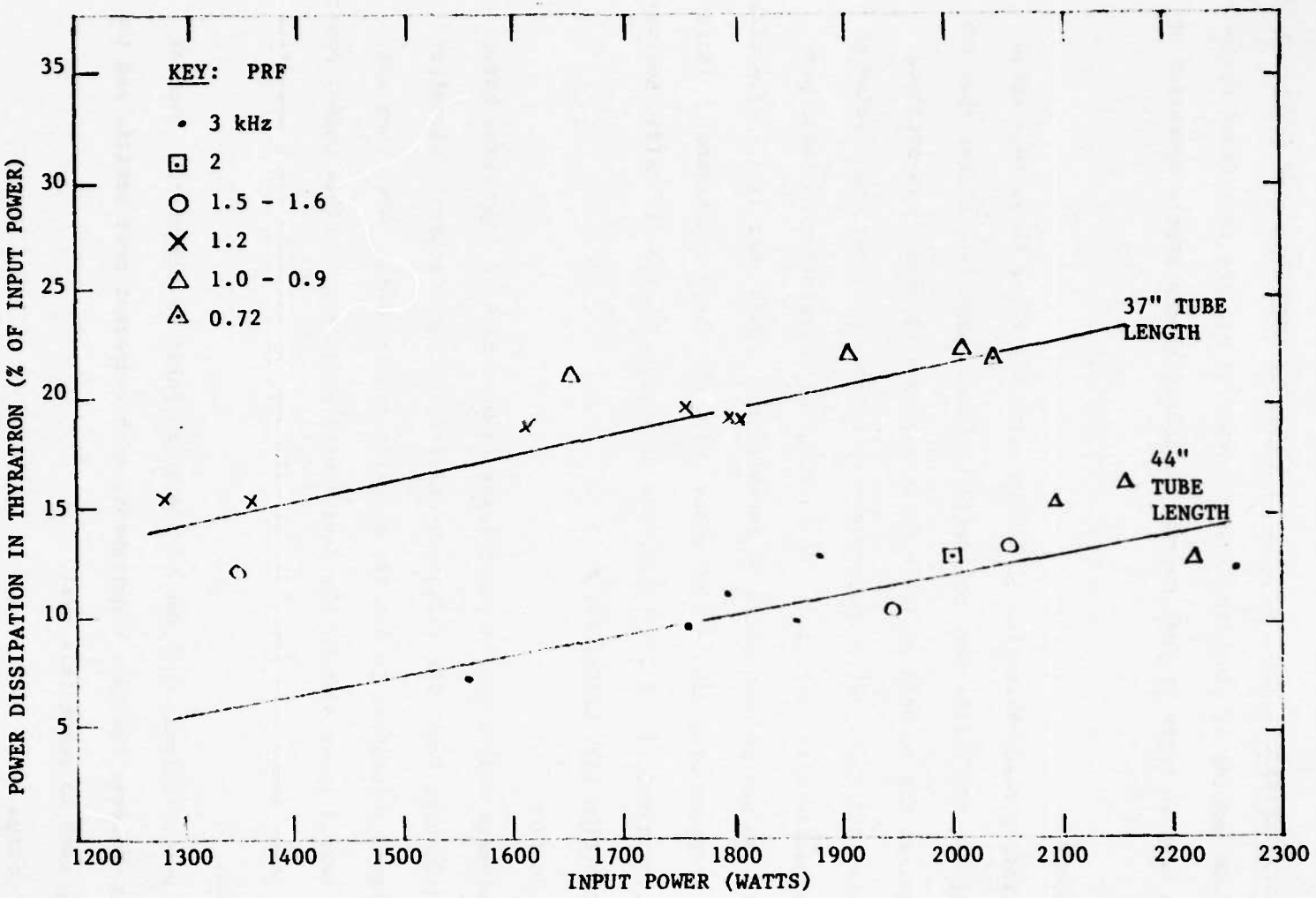

Figure 8. Energy Dissipation in EG&G 1802 Thyratron

Using this thyratron, peak currents in excess of 6000 amps were generated with no excess anode heating or discharge instability. Of all the thyratrons tested, this was the best in terms of peak current capabilities and stable operation at low rates.

5. Summary

The operating characteristics of lasers using all three thyratrons (EG&G 1802, EEV CX1174, ITT F-155) were dominated by laser parameters rather than the switch. Thus, as can be seen on Table 3, very good performance was obtained early with the 1802 (Nov. 1977) which was only reproduced later when radiation shield inadequacies were corrected. No substantial correlation of laser performance with the switch used could be established. (Note that 11.2 - 11.4 millijoules were produced with 2200 - 2400 watts using all three thyratrons). Improved reliability, particularly at low rates, was obtained with the ITT F-155, however.

3.3 LOW REPETITION RATE LASER DESIGN

3.3.1 Introduction

The discharge heated copper vapor laser is manufactured from three basic parts, the discharge tube, the radiation shields and the electronic circuitry. Each is designed separately to satisfy specific requirements. When they are combined to form a laser system, the device will produce a specific output power for a given input power. In addition, it will operate reliably for a specified time duration.

In the next sections, each one of the basic parts is discussed. Most of the analysis concerns specific requirements each component must satisfy and the final design used to reach this goal.

3.3.2 Tube Design

The laser tubes are made of AD-998 alumina with circular tantalum or stainless steel electrodes at each end as shown in Figure 9. At present, the electrodes

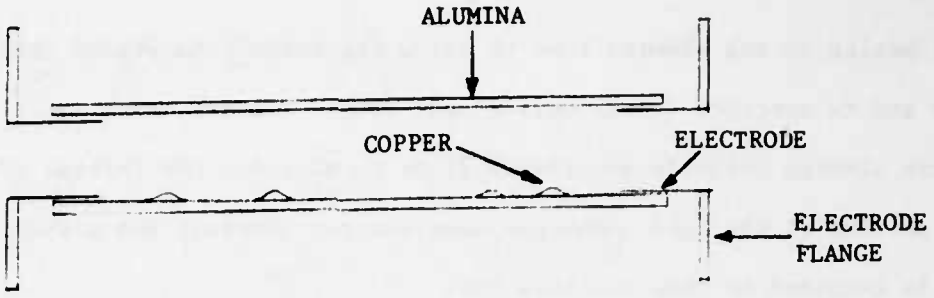

Figure 9. Standard Laser Tube and Electrodes

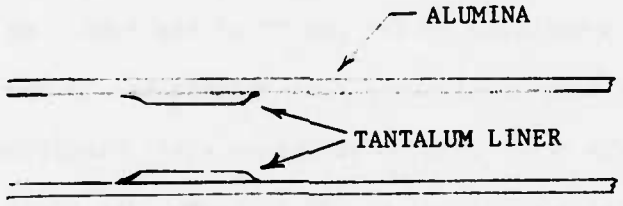

Figure 10. Copper Storage in Flared Liner Well

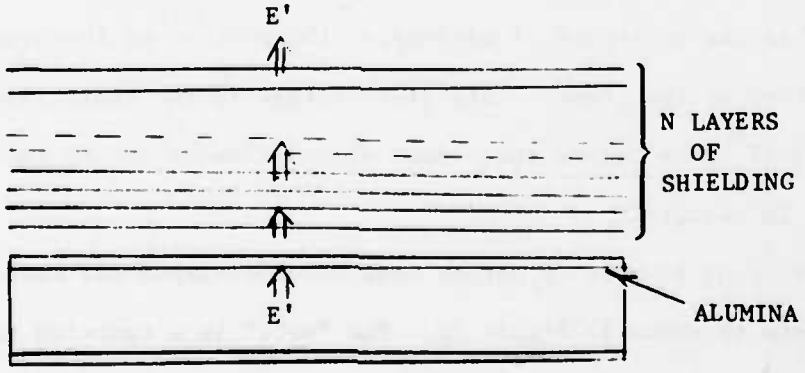

Figure 11. Thermal Radiation Shield Laser Configuration

are not sealed to the alumina tube to allow the ceramic to expand freely during heat up and to contract freely during cool down. The fit, however, at the electrode alumina joint is relatively tight to minimize the leakage of the buffer gas out of the tube. The gas does escape, however, and a small vacuum system is required to pump out this gas.

The choice of electrode material is determined by the alumina tube dimensions. Because of the poor tolerances maintained in casting the alumina tubes, there is considerable variations in inside and outside diameters. For example, the inside diameter of a 1½" ID standard tube may vary from slightly less than 1½" to 1/8" more. When the tube is slightly more than 1½", then a 1½" OD, 0.020" wall thickness tantalum electrode is inserted into the tube. In all other cases, a stainless steel electrode is machined to fit the OD of the tube. No experimental evidence exists to indicate superiority of either technique. In the 12 mJ/pulse laser discussed later in this report, an OD stainless steel electrode was used at the anode and an ID tantalum electrode at the cathode. The electrodes are then either pressed fitted or welded into stainless steel flanges. These flanges are bolted to the vacuum jacket using copper gaskets to complete the seal.

The copper is placed in these tubes in several ways. The first technique involves placing small beads along the entire length of alumina tube. In a typical experiment, 15 one gram beads are placed every 1½" down the bore of the tube. The method has the advantage of minimizing the portion of the cross sectional area blocked by the copper. Its disadvantage is its short lifetime which is only 7 and 10 hours before the copper vapor diffuses out of the laser tube and reloading is required.

Two techniques using sources of copper have been developed and successfully tested. One of these is shown in Figure 10. The "wall" is a tantalum tube flared at both ends and inserted into the discharge tube. The copper is located

between the inside surface of the alumina tube and the tantalum and evaporates through a small hole in the tantalum. Three of these are put in each discharge tube with enough copper to last 30 to 50 hours.

A third technique uses an alumina source tube filled with copper which is inserted into the discharge tube. Sufficient copper to last over 100 hours is available with this design. The only drawback to this technique is the sizeable portion of the discharge tube blocked by this source. This limit to the active volume can be compensated for by increasing the size of the main alumina tube.

The results of long life experiments conducted under other programs[24,25] are summarized in Table 4.

Table 4

Lifetime Characteristics of Copper Vapor Laser Tubes
Using Various Storage Techniques

Metal Storage Description	Mass Stored	Power Temperature	Lifetime	Comments
Beads	1 gm	7W (6 kHz) 1520°C	1½ hrs.	Reference 24
	24 gm	10W (1 kHz) 1550°C	10½ hrs.	This program, two fills copper remaining at end
Liner	13 gm	7W (6 kHz) 1450°C	55 hrs.	Reference 24
Reservoir Tube	194 gm	15W (6 kHz) ~1500°C	215 hrs.	References 24, 25

Discharge tubes using beads and a small source were tested in this program without any significant problems. Table 4 gives the data for one of these.

24. R. S. Anderson, et al, Air Force Avionics Lab Contract F33615-76-C-1137.

25. R. S. Anderson, et al, ERDA Lawrence Livermore Laboratory Contract 5949703.

In addition to the copper vapor, the discharge tube contains a few torr (2-4) of helium as a buffer gas. It is needed to help sustain the discharge while at the same time reducing the diffusion of copper out of the hot zone. As stated above, the helium slowly leaks out of the tube and so has to be continually resupplied. When a sealed off tube is made, this requirement will be eliminated.

3.3.3 Thermal Radiation Shield

Surrounding the alumina tube is a multi-layer thermal radiation shield designed to regulate the operating temperature of the laser. With the proper shield design, a discharge tube will rise to and remain at a given temperature for a given input power. Two physical parameters govern the radiation shields effectiveness. They are the number of layers of shielding and the emissivity of each layer. In the sample shield shown in Figure 11, there are N layers all with emissivity ε. The power input per unit length is E' which is proportional to the input power E coming from the main power supply.

Shield #1 is the last shield before the outer vacuum jacket which is at a temperature T_0. Assuming minimal conduction losses, the power radiated at equilibrium to the vacuum jacket (E') is given by:

$$E' = \varepsilon\sigma \left[A_1 T_1^4 - A_0 T_0^4\right] \tag{1}$$

or

$$A_1 T_1^4 = \frac{E'}{\varepsilon\sigma} + A_0 T_0^4 \tag{2}$$

where ε is surface emissivity, A_i is the shield or jacket area per unit length, σ is the Stefan-Bottzman constant and T_i is the approximate temperature.

Likewise the power radiated at equilibrium from shield #2 to shield #1 is E' and is given by:

$$E' = \varepsilon\sigma \left[A_2 T_2^4 - A_1 T_1^4\right] \tag{3}$$

or

$$A_2 T_2^4 = \frac{2E'}{\varepsilon\sigma} + A_0 T_0^4 \tag{4}$$

Continuing this mathematical progress, an expression for T_N^4 can be computed.

$$A_N T_N^4 = \frac{NE'}{\varepsilon\sigma} + A_0 T_0^4 \tag{5}$$

$$T_N = \left[\frac{NE'}{\varepsilon\sigma A_N} + \frac{A_0}{A_N} T_0^4\right]^{1/4} \tag{6}$$

For the discharge tube used in the experimentation, the parameters listed below can be substituted into equation 6 and values of T_N computed for different input powers.

T_0 ≡ outer jacket temperature 370°K

A_0 ≡ outer jacket area/length 20 cm^2

A_N ≡ discharge tube area/length 14 cm^2

σ = 5.67 x 10^{-12} watts/cm^2 - $(°K)^4$

ε = 0.1 to 0.4

The results of these calculations are shown in Figures 12, 13, 14, and 15.

For the discharge heated lasers used in these experiments a 22 layer radiation shield with emissivity ∿ 0.3 has been used. Using Figure 15, which was derived from Figures 12, 13 and 14, between 1500 and 2000 watts of input power are needed for the tube to reach its proper operating temperature. This agrees with the experimentation measurements made on this system.

The innermost eight layers of the radiation shields, which are the hottest, are made of molybdenum foil and are separated by an alumina batting marketed under the name "Saffil". This material has very low thermal conductivity when it is a loose weave and not densily packed. It also prevents the different layers of molybdenum from touching and bonding together by thermal diffusion.

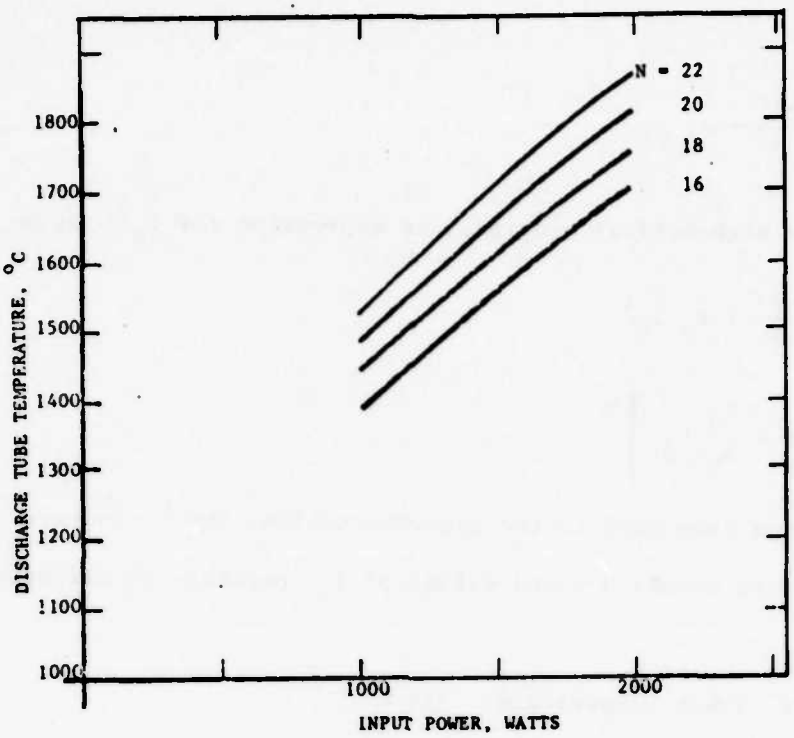

Figure 12. Discharge Tube Temperature As A Function of Input Power Shield Emissivity: $\varepsilon = 0.2$, N is the number of shields

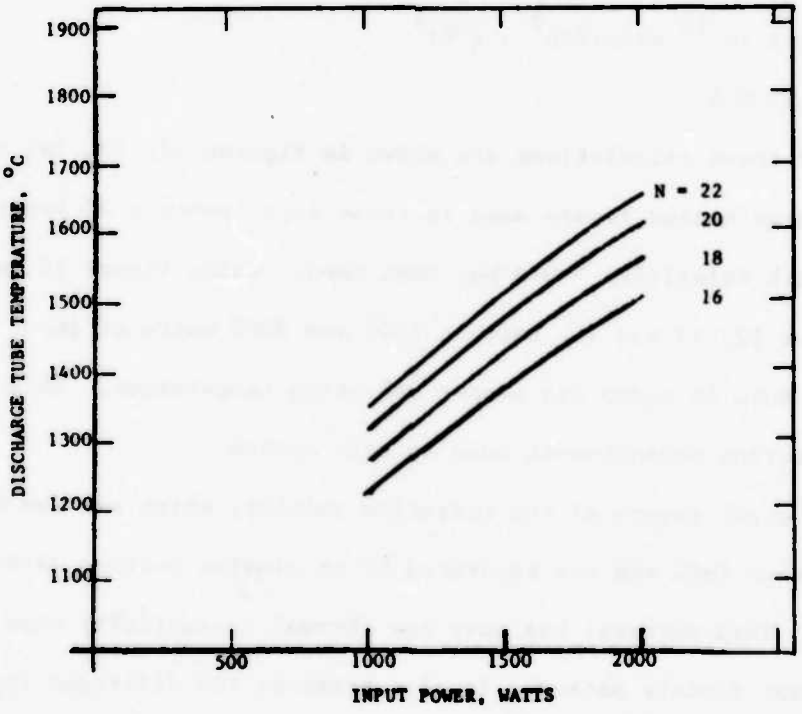

Figure 13. Discharge Tube Temperature As A Function of Input Power Shield Emissivity: $\varepsilon = 0.3$, N is the number of shields

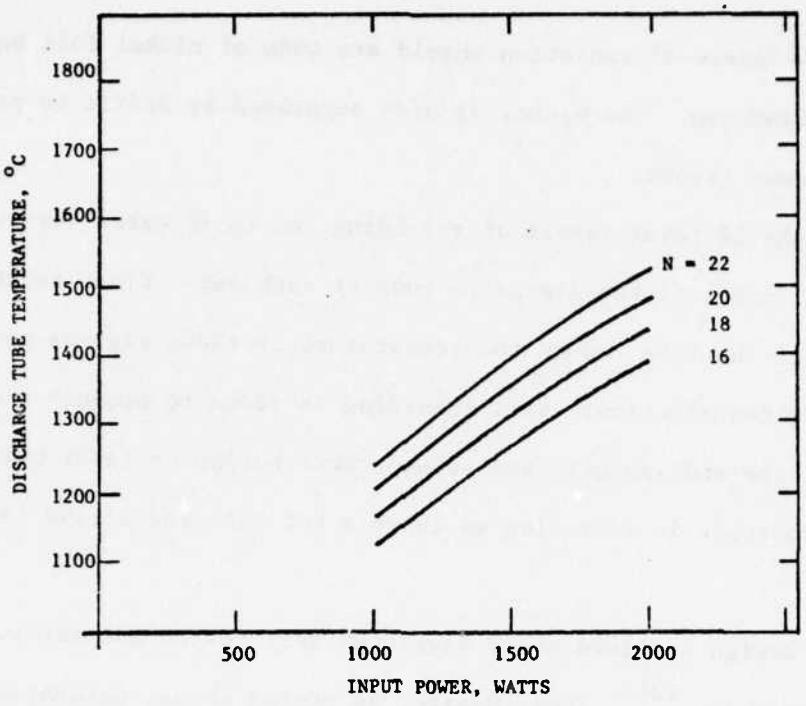

Figure 14. Discharge Tube Temperature As A Function of Input Power Shield Emissivity: $\varepsilon = 0.4$, N is the number of shields

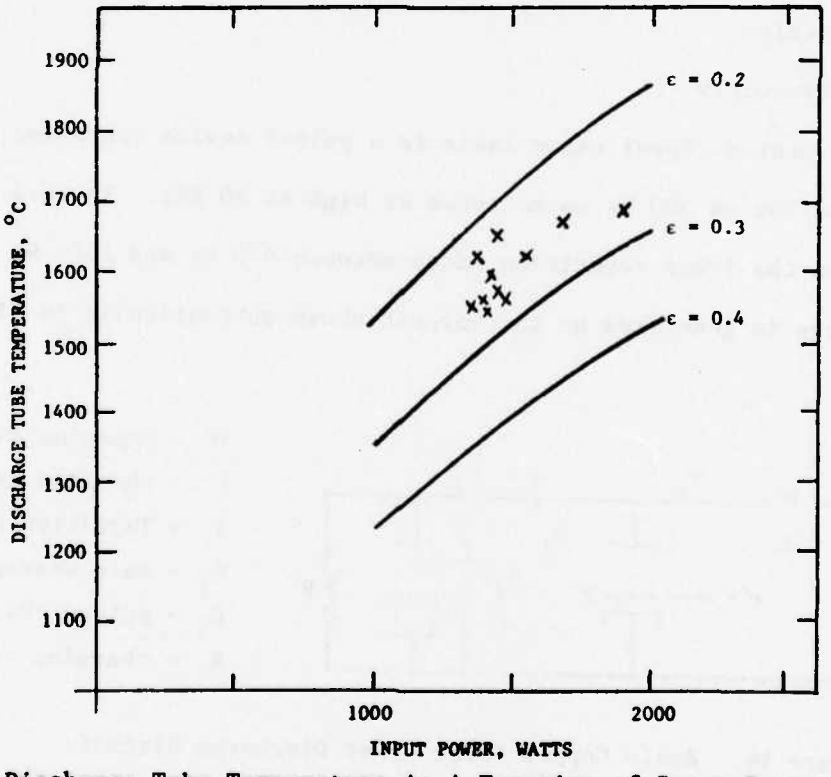

Figure 15. Discharge Tube Temperature As A Function of Input Power. Thermal Radiation Shield is Composed of 22 Layers. Experimental points, x, indicate average emissivity of $\varepsilon = 0.25$

The remaining 14 layers of radiation shield are made of nickel foil because of the expense of molybdenum. The nickel is also separated by Saffil to prevent bonding between adjacent layers.

In addition to the 22 total layers of shielding, up to 10 extra layers surround the last 12 inches of the discharge tube at each end. Since radiation losses out the ends of the tube reduce the temperature in these regions and minimize their lasing contribution, extra shielding is added to produce a more uniform temperature tube and increase the volume contributing to laser output. This technique is important in achieving as large a hot zone and active laser volume as possible.

Shields of the design outlined above have been well tested and survive for over 100 hours of operation.[24] Their design, as stated above, determines the ultimate operating conditions of the laser and hence is one of the most important components of the device.

3.3.4 Electronic Circuitry

The discharge heated copper vapor laser is a pulsed device operating at repetition rates as low as 500 Hz up to rates as high as 20 kHz. In this program, the emphasis was on the lower repetition rates between 500 Hz and 1500 Hz. The electrical discharge is generated by the circuit shown schematically in Figure 16 below.

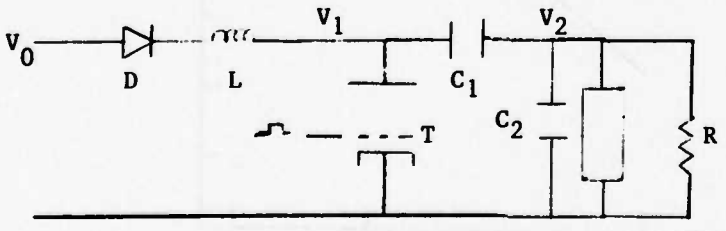

D - charging diodes
L - charging inductors
T - Thyratron switch
C_1 - main storage capacitor
C_2 - pulsed charge capacitor
R - charging resistor

Figure 16. Basic Copper Vapor Laser Discharge Circuit

Capacitor C_1 is resonantly charged through the diode and inductor series circuit. At first $V_1 = 2V_0 = V_1$ (initial). When the thyratron is turned on by a trigger pulse, V_1 falls rapidly toward zero while V_2 falls toward $-V_1$ (initial). Charge is transferred from C_1 to C_2 until V_2 reaches the breakdown voltage of the laser tube. At this time both C_2 and C_1 discharge through the tube. Because of stray circuit inductance, V_1 goes negative to a final value $V_1 = -V_f$. The thyratron turns off leaving a voltage across L of $V_0 + V_f$. During recharge, the voltage on C_1 swings a total of 2 $(V_0 + V_f)$ up to a final value of $2(V_0 + V_f) - V_f$ or $2V_0 + V_f$. The discharge process then repeats itself.

Figure 17 shows the voltage waveform at V_1. In this case, the anode starts at -4.5 KV and recharges to 17 KV for a total voltage swing of 21.5 KV. The decay of this voltage during the interpulse period can be avoided by using a larger inductor in the charging circuit. This increases the recharge time and hence reducing the time for this voltage decay.

Figure 18 shows the voltage at V_2. Initially the voltage falls to -13 KV in 100 nsec at which time the tube breaks down. It takes 70 nsec for this voltage to fall to zero. It then swings negative due to the discharge circuit inductance. Measurements made on the deposition of energy into the tube indicate that nearly all of it goes in during this first 70 nsec. The laser pulse usually terminates at this time or less than 5 nsec later.

For efficient lasing to occur, the current discharge pulse must have a fast rise time (40 - 50 nsec) and a short FWHM (40 - 50 nsec). The inductance of the circuit totally governs these two time periods. By reducing this inductance, a faster rising, shorter current pulse excites the copper vapor producing a higher output pulse energy. A systematic study of different techniques to minimize the circuit inductance was discussed earlier in Section 3.2.2. As shown there,

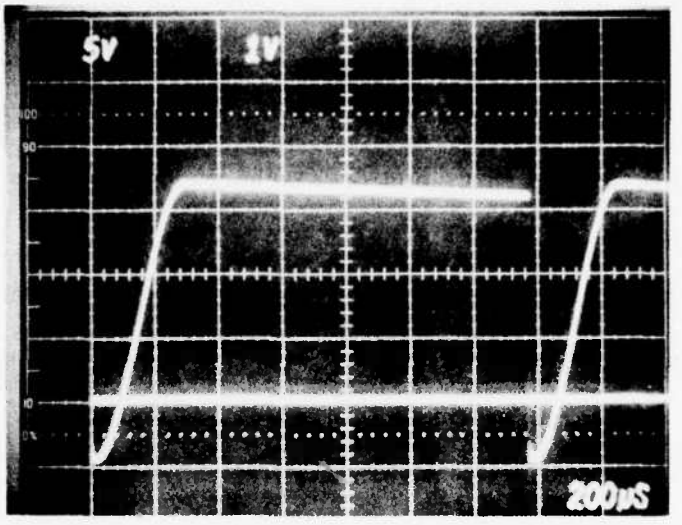

Figure 17. Thyratron Anode Voltage

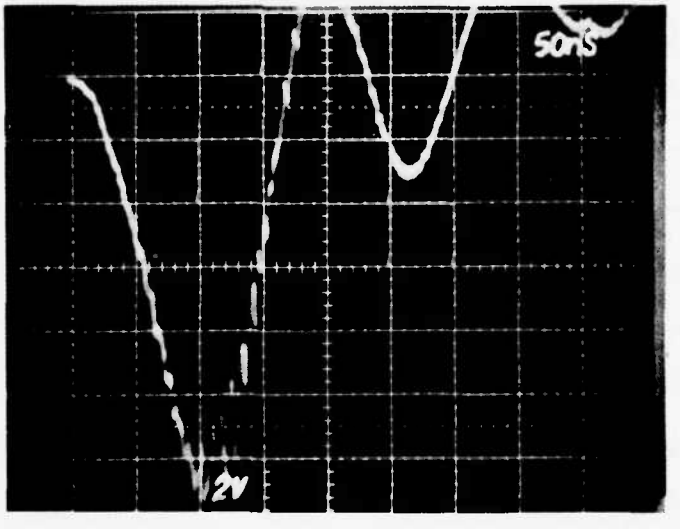

Figure 18. Voltage Across Laser Tube

the ease of implementation and the acceptably efficient performance of the pulse charge capacitor made it the preferred mode of operation for the laser tests in this program.

3.4 LARGE DIAMETER LASER TUBE TEST

3.4.1 Introduction

At the beginning of this program, it was decided that the main experimental effort would be a volumetric scaling of the existing discharge heated copper vapor laser. No new unique designs of laser tubes or discharge circuitry would be tried. It was a program intended to see how far the present system could be extended.

Coupled with this volumetric increase, however, was a program investigating different electrical components for the discharge circuitry. That is, different thyratrons and higher voltage rating capacitors were to be tested for lifetime, stability, and efficiency. These components were to be substituted for the existing components in the discharge circuit as opposed to designing totally new circuits. Again, this plan fitted into the concept of seeing how much more the existing system could produce.

Starting with this objective, three different length 1" ID tubes were evaluated followed by two different lengths 1¼" ID tubes. Finally a 1½" ID tube was assembled and tested. This latter tube produced the highest energy/pulse, but it was not optimized, nor can it be inferred to be the optimum tube that could be used in this program.

In conjunction with this, capacitors manufactured by Condenser Products were tested for high voltage (25 kV) at low repetition rates (500 to 1000 Hz) with no failures over the duration of the program. The capacitance used for essentially all discharge tubes varied from 6 nf (main capacitor) - 1 nf (pulse charged capacitor) at 6 kHz to 25 nf - 9 nf at about 1 kHz. The voltage was raised at the lower rates and so the input power could be maintained constant over the whole

range. Three different thyratrons, EG&G 1802, EEV CX 1174, and ITT F-155 were also tested. The results of their evaluation were presented in Section 3.2.2.

The following sections discuss each of these tube sizes and gives the experimental results. In all cases the average power of the laser was measured using a Scientech Model 36-0401 calorimeter and the laser pulse shapes were detected by a Hammumatsu photo diode and displayed on a Tektronix 7904 oscilloscope. The relative intensities of the 5105 Å and the 5782 Å lasing transitions were determined by separating the beam with a grating blazed at 5500 Å and measuring the average power on the Scientech calorimeter. At the same time, the temporal pulse of each transition shape was measured using the photo diode.

3.4.2 1" ID Discharge Tubes

The first discharge tube tested in this program had a 1" ID and was 29.5" long from flange to flange. The radiation shields covered 25.5" of this length making the effective "hot" zone between 10" and 20" long.

The effective "hot zone" is determined by the volume defined by the copper deposition sites. After a tube has been operated for some time, copper is observed to have deposited at each end of the tube. At the anode end the deposition is usually 8" to 10" inside the end of the radiation shield. At the cathode end the deposition is usually 8" to 10" from the electrode flange. This has been observed for all three tube diameters discussed in this section. The volume bounded by these deposition sites is defined as the effective hot zone.

The discharge tube operated at repetition rates as low as 1.5 kHz and was not tested any lower because of discharge instabilities. The energy/pulse results for the tube are shown in Figure 19.

When the same diameter tube was increased in length to 37.75", the output energy/pulse increased from 3.56 mJ/pulse at 1.5 kHz to 6.3 mJ/pulse, or by a factor of 1.8 (see Figure 19). In this tube, the radiation shields covered 33" of the

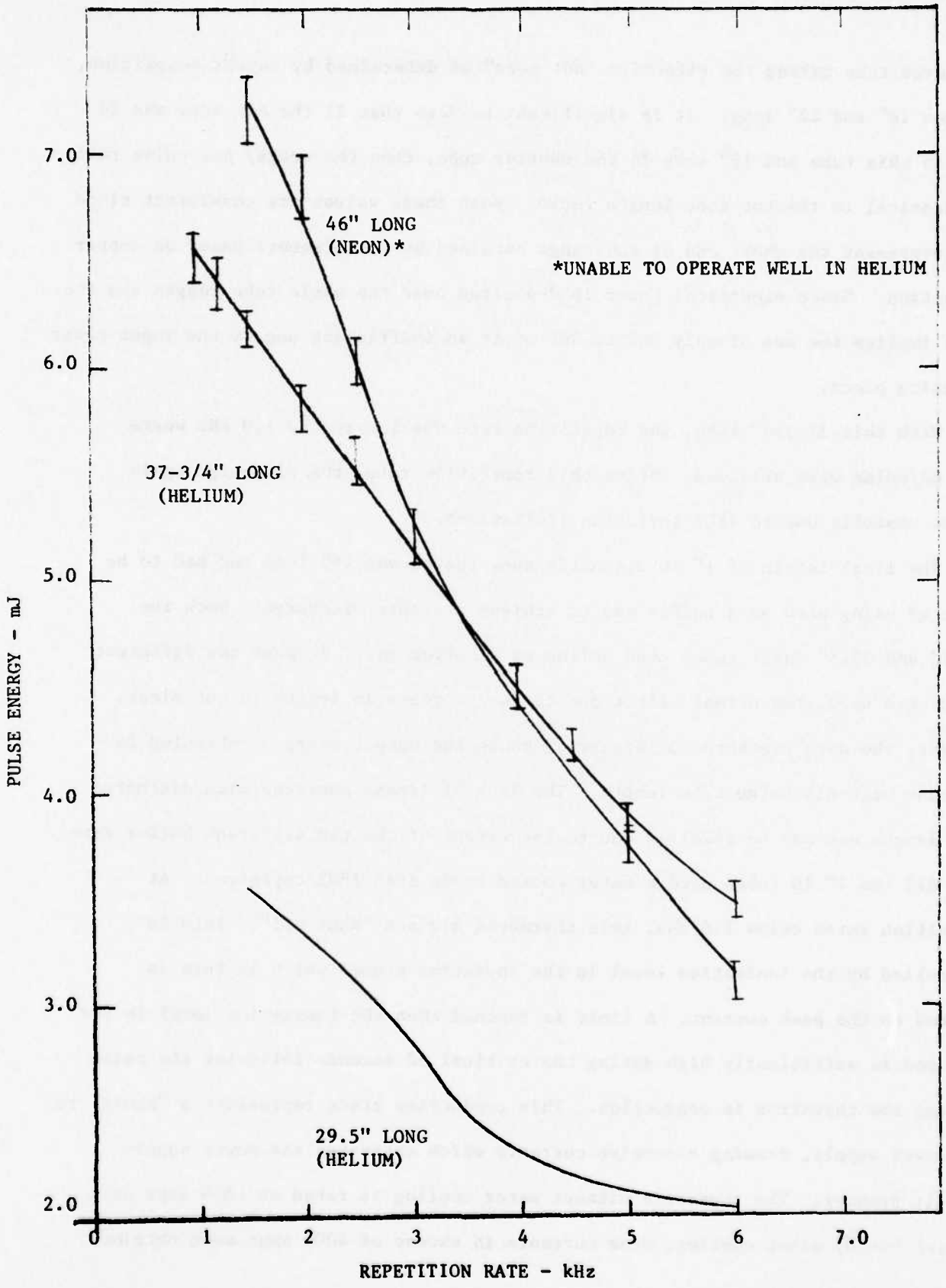

Figure 19. Pulse Energy For 1" ID Discharge Tube As A Function of Repetition Rate

discharge tube making the effective "hot zone" as determined by copper deposition, between 18" and 22" long. It is significant to note that if the hot zone was 18" long in this tube and 10" long in the shorter tube, then the energy per pulse ratio is identical to the hot zone length ratio. Both these values are consistent since they represent the short end of the range obtained by measurements based on copper deposition. Since electrical power is deposited over the whole tube length and the above implies the use of only 39% to 48% of it an inefficient use of the input power is taking place.

With this 37-3/4" tube, the repetition rate was lowered to 1.0 kHz where 6.56 mJ/pulse were obtained. Below this repetition rate, the discharge again became unstable due to 1802 thyratron limitations.

The final length of 1" ID discharge tube tested was 46" long and had to be operated using neon as a buffer gas to achieve a stable discharge. Both the 37.75" and 29.5" laser tubes used helium as a buffer gas. Because two different gases were used, the actual effect due to the increase in length is not clear. However, the data presented in Figure 19 shows the output energy continuing to increase with discharge tube length. The lack of linear increase with discharge tube length can not be resolved due to the effect of the two different buffer gases.

All the 1" ID tubes used a water cooled anode EG&G 1802 thyratron. At repetition rates below 1.0 kHz, this thyratron did not "shut off". This is controlled by the ionization level in the thyratron plasma which in turn is related to the peak current. A limit is reached when the ionization level in the hydrogen is sufficiently high during the critical 50 seconds following the pulse to keep the thyratron in conduction. This conduction state represents a "short" to the power supply, drawing excessive currents which activates the power supply circuit breaker. The thyratron without water cooling is rated at 1500 amps peak current but by water cooling, peak currents in excess of 4000 amps were obtained.

This limit was reached at about 1 kHz.

3.4.3 1¼" ID Discharge Tube

Two 1¼" ID tubes were tested. The results are shown in Figure 20. As with the 1" ID tube, increasing the length from 29.5" to 37.75" produces a significant increase in pulse energy. For the 1¼" tube, it is a factor of 1.7 compared to 1.8 for the 1" tube. No attempt was made to operate a 46" long 1¼" ID tube, but clearly this should be done in the future. In this experimental program, however, it was decided to go directly to a 1½" tube 46" long which is discussed in the next section.

Comparing Figures 19 and 20, the effect of scaling the discharge tube diameter can be seen. For example, with a 29.5" long tube operating at 2.5 kHz, the 1¼" diameter tube produced 5.1 mJ/pulse compared to 3.6 for the 1" tube. This is a factor of only 1.42 compared to a factor of 1.56 increase in cross sectional area. With the 37.75" long tube operating at 1.0 kHz, the 1¼" tube produced 9.3 mJ/pulse compared to 6.5 mJ/pulse for a 1" tube. This is only a factor of 1.43 indicating that the output power does not quite scale linearly with the discharge tube cross sectional area. However, in section 4.1 it is shown that when the input energy per unit volume is considered, then the laser output energy does scale linearly with cross sectional area. Unfortunately no data is available comparing 1½" ID tube to 1¼" or 1" tubes of comparable lengths.

3.4.4 1½" ID Discharge Tubes

After comparing the results of scaling both the tube lengths and cross sectional area, it was decided to built a 1½" ID tube 45" long. This was both the largest diameter and longest tube tested in the program and it produced the highest pulse energy ever obtained from a copper vapor laser. At 1.0 kHz, 12.12 mJ/pulse was obtained from this laser at a "wall plug" efficiency of 0.41%. The data for this tube showing the effect of repetition rate on pulse energy is shown in Figure 21.

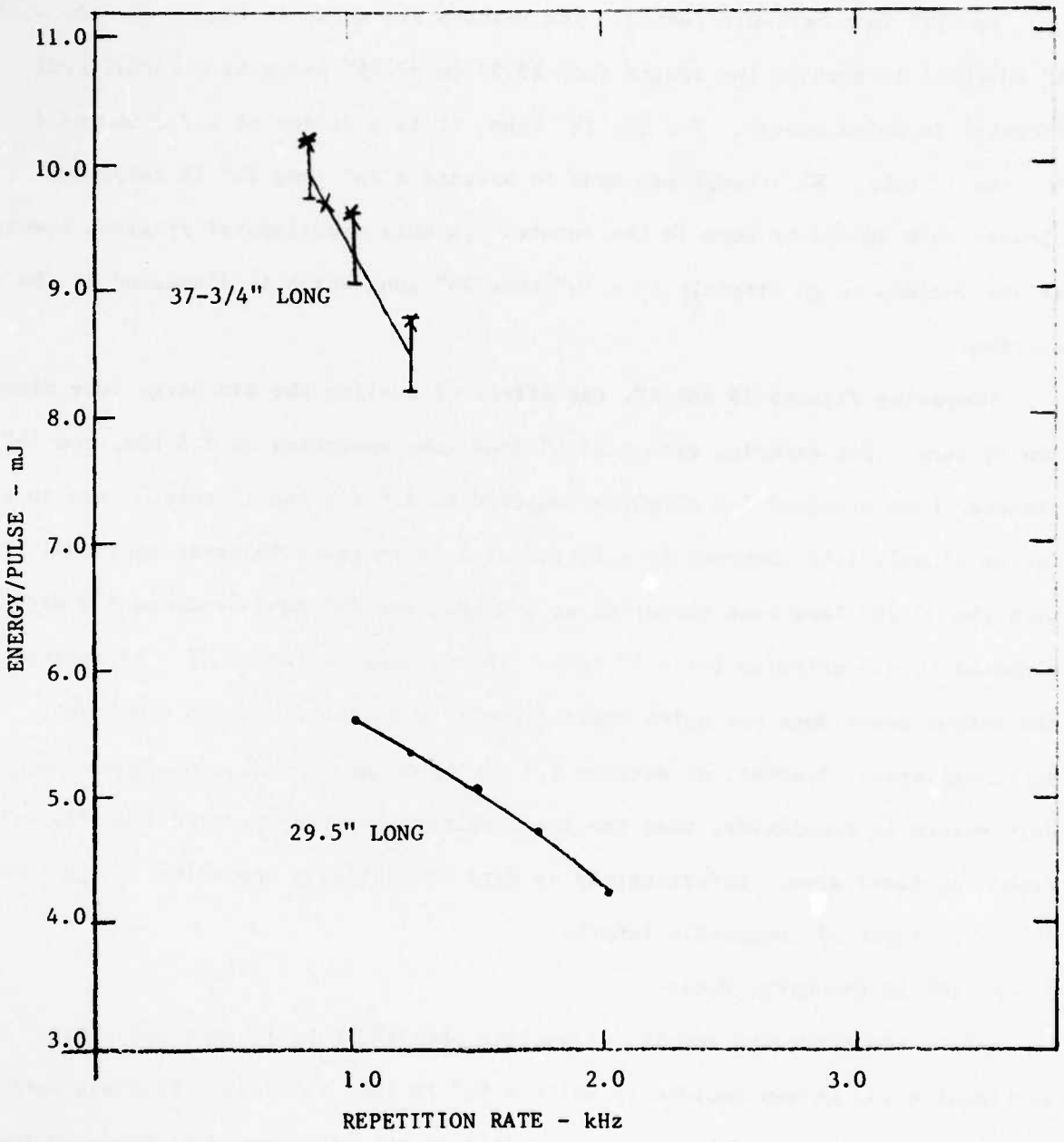

Figure 20. Pulse Energy For 1¼" ID Discharge Tube As A Function of Repetition Rate

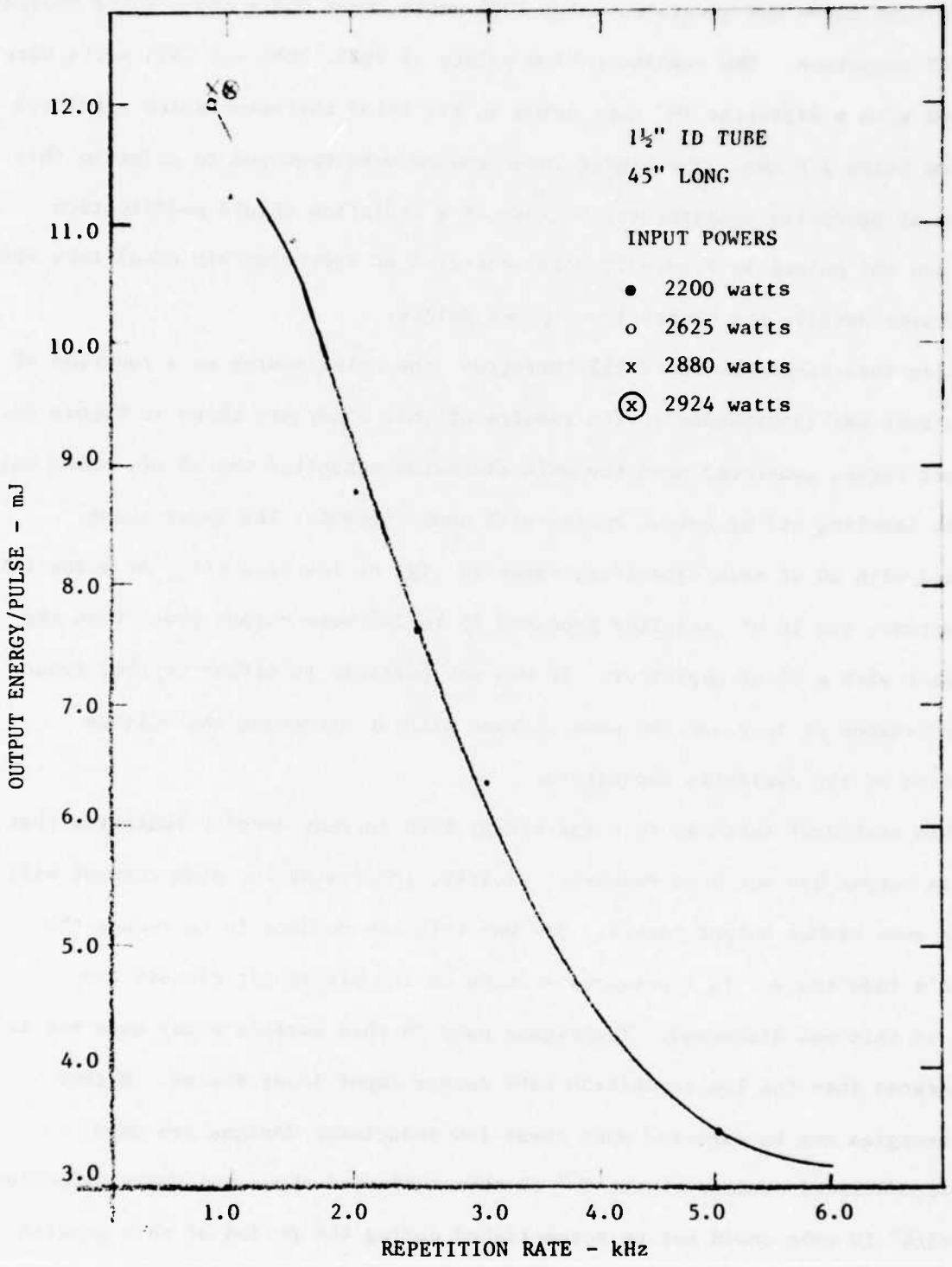

Figure 21. Pulse Energy For 1½" ID Discharge Tube As A Function of Repetition Rate

The main curve was generated using 2000 watts input power and a water cooled EG&G 1802 thyratron. The remaining five points at 2625, 2880 and 2924 watts were generated with a different 1½" tube using an ITT F-155 thyratron which permitted operation below 1.0 kHz. The higher input powers were required to maintain this new tube at operating temperatures because of a radiation shield modification. Hence, all the points in Figure 21 were generated at approximately equal tube operating temperatures despite the higher input power points.

Using this tube with the F-155 thyratron, the pulse energy as a function of peak current was investigated. The results of this study are shown in Figure 22. The lower curve, generated when the main discharge capacitor was 25 nf, shows only a slight leveling off of output energy with peak current. The upper curve, generated with 20 nf main capacitor, shows no sign of leveling off. At a specific peak current, the 20 nf capacitor produced 15 to 20% more output power than the same laser with a 25 nf capacitor. It was not possible to either further reduce the capacitance or increase the peak current without exceeding the voltage limitation of the available capacitors.

This continual increase in pulse energy with current density indicates that the limit in output has not been reached. Clearly, increasing the peak current will produce even higher output powers. One way this can be done is to reduce the circuit's inductance. In a previous section on the electronic circuit the effect of this was discussed. Techniques used in this earlier study have yet to be incorporated into the low repetition rate copper vapor laser design. Higher pulse energies can be expected when these low inductance designs are used.

The continued studies of the 1½" ID tube indicated above and their extension to a 1-3/4" ID tube could not be accomplished during the period of this program due to the late availability of the large diameter facility.

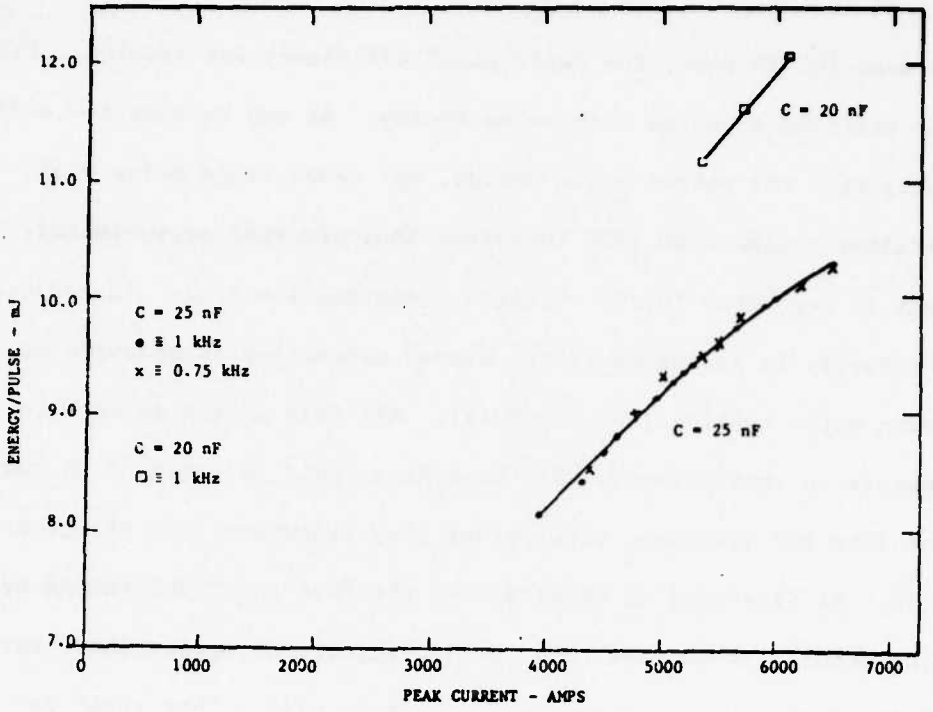

Figure 22. Pulse Energy For 1½" ID Discharge Tube As A Function of Peak Current

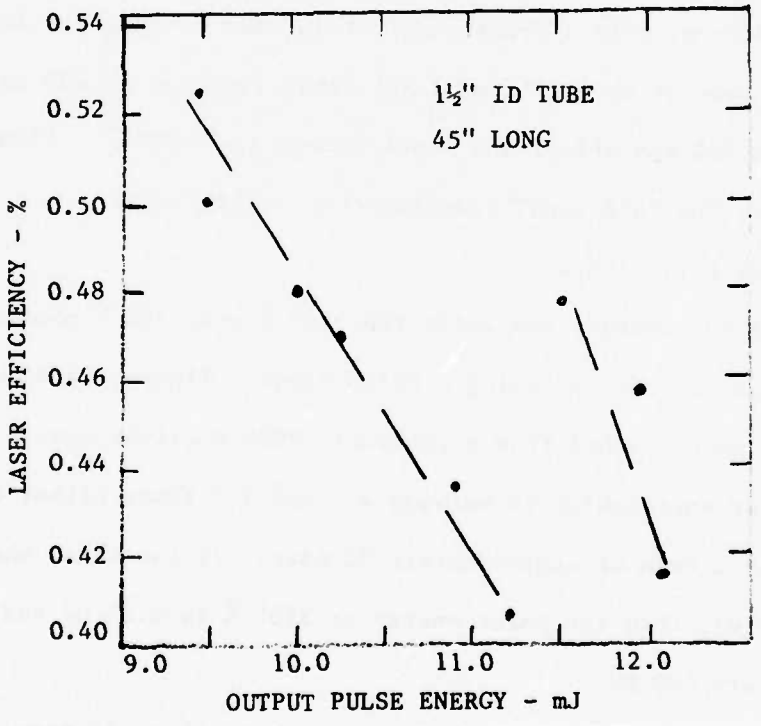

Figure 23. Efficiency of a 1½" ID Discharge Tube As A Function of Pulse Energy

Using this same 1½" ID tube, the "wall plug" efficiency was studied. Figure 23 shows how the efficiency varies with pulse energy. As can be seen the efficiency does fall slightly with the output pulse energy, but never drops below 0.4%. Studies using a water cooled EG&G 1802 thyratron indicate that approximately 12 to 22% of the energy is deposited in the thyratron (see Section 3.3). In addition 14 to 20% of the energy is deposited in the window assemblies as measured by calorimeters using water cooling (see Appendix). All this energy is lost to the laser and represents an inefficiency. If the system could be designed so that this energy went into the discharge tube rather than elsewhere, the efficiency would approach 1%. As discussed in Section 3.4, the "hot zone" determined by where copper deposition occurs, is shorter than the interelectrode separation. For example, the 12.12 mJ per pulse was obtained in a tube with a "hot zone" 24" to 28" long while the interelectrode distance was 44". Since energy is deposited over this larger distance, only a fraction of it is used to pump the laser transition. In the case of the 12.12 mJ laser, this fraction is 45% to 64%, meaning that between 36% and 46% of the input energy is "wasted". Clearly improved design could increase the "hot zone" reducing this inefficiency.

3.4.5 Laser Temporal Pulse Shape

Using a grating to separate spatially the 5105 Å and 5782 Å beams, the temporal behavior can be detected using a photo diode. Figures 24 and 25 show both transitions as photographed from a Tektronix 7904 oscilloscope.

The 5105 Å laser pulse which is between 2.1 and 2.3 times higher energy than the 5782 Å pulse has a FWHM of approximately 32 nsec. If the total energy per pulse in both lines is 12 mJ, then the pulse energy at 5105 Å is 8.25 mJ and the peak power is approximately 250 KW.

The 5782 Å laser pulse has a FWHM of approximately 20 to 25 nsec. At 12 mJ total pulse energy, its peak power is approximately 150 KW. The total peak

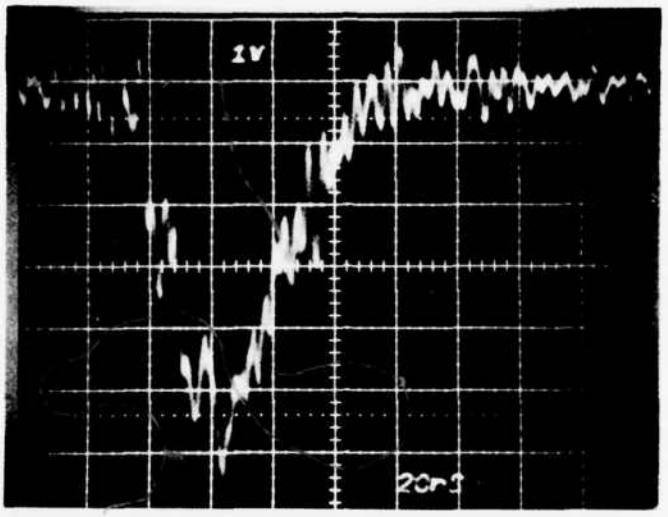

Figure 24. 5105Å Pulse

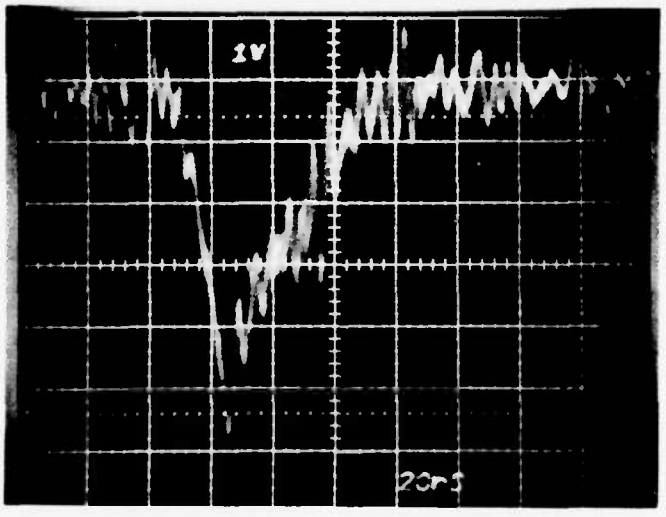

Figure 25. 5782Å Pulse

power from both transitions is 0.4 MW. This is the highest ever obtained from a copper vapor laser.

Higher peak powers can be achieved by reducing the discharge current pulse width. At present the relatively long laser pulses, especially at 5105 Å, are due to the long current pulses. The total time of lasing for the 5105 Å line is 70 nsec which also is the time it takes the voltage across the tube to fall to zero from its breakdown value (see Figure 18 in previous section). When this time is reduced, the laser pulse is shorter and hence the peak power is also higher provided the pulse energy remains constant. It has generally been observed that the pulse energy will actually increase with faster discharge times leading to even higher peak powers.

3.4.6 Life Test

As discussed under the section on tube design, the technique currently used to extend the operating lifetime of the laser is to use some kind of source of copper. In the 1½" ID tube, a hollow alumina rod with an OD of 7/16" was filled with 30 gms of copper and slid into the laser. Using an input power of 2350 watts, this laser operated at over 10 mJ/pulse for four hours when the experiment was stopped due to a discharge tube failure. The tube itself had operated for longer than 10 hours and the failure was related to a poor electrode design which has since been solved during laser lifetime studies performed under other programs.[24, 25] No effort was made to start a second test since the program had ended and all alumina materials had been used. Nevertheless, the source technique will work for this low repetition rate laser and long lifetimes can be expected.

3.5 MOPA

One task of this program was to demonstrate the operation of a master oscillator power amplifier (MOPA) laser system at the desired low repetition rates. Once the practicality of this type of system was shown, then two 25 millijoules modules

could be coupled together as a master oscillator power amplifier (MOPA) to produce at least a 50 millijoule pulse laser. Although this last step was not completed, the demonstration of a MOPA system at low repetition rates was successfully accomplished.

Figure 26 is a schematic of a MOPA system. Basically, it consists of a high power oscillator laser which is optically coupled into a second gain medium which subsequently amplifies this incoming signal. For very high small signal gain media such as strongly superfluorescent copper vapor, the presence of the optical field from the oscillator prevents any parasitic modes from developing in the amplifier. This means the MOPA system potentially can emit higher pulse energies than the sum of the two pulse energies when the oscillator and amplifier are operated separately as two oscillators. This effect has been demonstrated with copper in this laboratory[1] and hydrogen fluoride at Los Alamos.[26] In this case, two 25 millijoule modules would produce more than 50 millijoules if operated as a MOPA. However, if the gain of the amplifier is relatively low so that parasitic losses are low, the most that can be expected from the MOPA is simple addition of the pulse energies of the two modules.

The MOPA system shown in Figure 26 was tested at a repetition rate of 2.0 kHz. The oscillator was a 7/8" ID alumina tube with a flange to flange separation of 29.5". At 2.0 kHz, it emitted 1.85 $\pm$ 0.15 millijoules per pulse through the amplifier. That is, with the amplifier turned off, the output pulse energy from the oscillator after it had been coupled through the amplifier was 1.85 $\pm$ 0.15 millijoules.

The amplifier was the same length as the oscillator, but was a 1" ID alumina tube. When used as an oscillator by placing it in a optic cavity, this laser emitted 3.4 $\pm$ 0.2 millijoules per pulse at 2.0 kHz. Thus, if the pulse energies

26. R. W. Getzinger, N. R. Greiner, K. D. Ware, J. P. Carpenter and R. G. Wenzel, IEEE J. Quan. Elec. QE-12, 556, (1976).

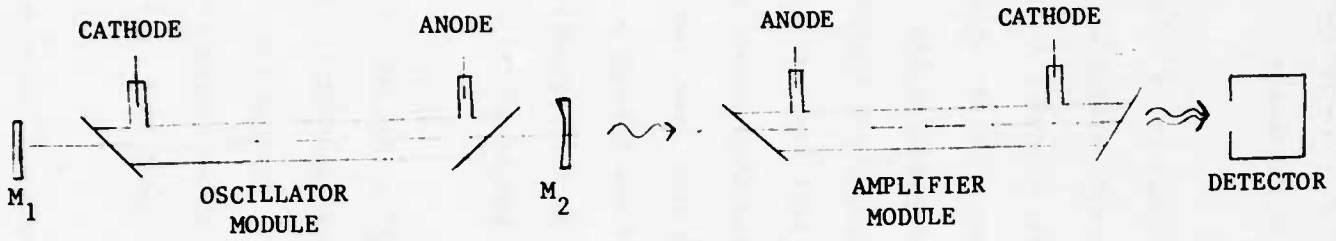

Figure 26. MOPA Configuration for Individual Modules

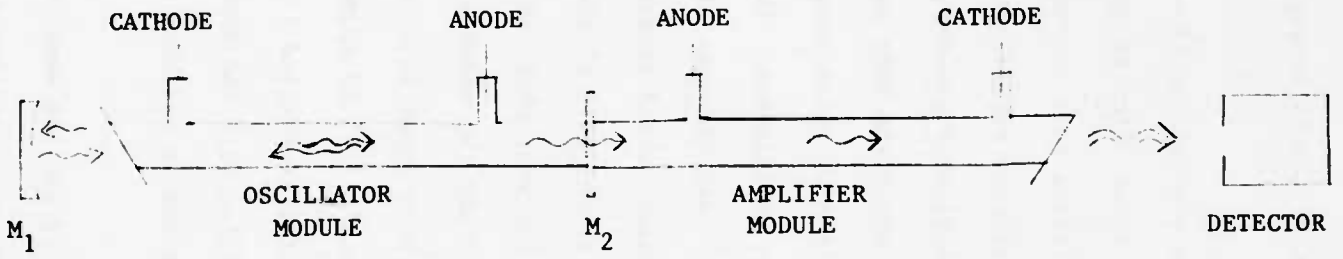

Figure 27. MOPA Configuration for Connected Modules

from the two lasers were added, the total output pulse energy at 2.0 kHz would be 5.25 $\pm$ 0.35. When operated as a MOPA, however, the output pulse energy was 5.85 millijoules or 11 $\pm$ 7% more than the algebraic sum. Any extra pulse energy must be coming from atoms which normally emitted photons in directions other than along the optic axis. The presence of the high optical field from the oscillator in the amplifier stimulated these atoms to emit along the optic axis and hence contribute to the laser pulse.

This same MOPA was operated at 2.5 kHz where the oscillator emitted 1.7 $\pm$ 0.1 millijoules and the amplifier 3.25 $\pm$ 0.13 millijoules. This algebraically adds to between 4.7 and 5.2 millijoules. When operated in a MOPA system, 5.38 millijoules were obtained representing between 7 $\pm$ 4% increase in total pulse energy.

A second type of MOPA system, shown in Figure 27, in which the two lasers are bolted together was also tested. This eliminates two of the brewster angle glass windows since the one window between the two lasers now serves as an output mirror for the oscillator and an input coupling window for the amplifier.

Using this system with the same discharge tubes used in the first MOPA system, 6.23 millijoules per pulse was obtained at 2.0 kHz and 5.68 millijoules per pulse at 2.5 kHz. This is approximately a 6% increase over the separate configuration shown in Figure 26.

No other MOPA work was done during this program since the main emphasis shifted to the development of the 25 millijoule per pulse module. The work which was outlined above, however, was sufficient to demonstrate that MOPA systems could be operated at low repetition rates and, more importantly, that at least addition of the pulse energies of the component modules can be realized. This is a very important fact to be considered when designing the final 50 millijoules per pulse copper vapor laser.

SECTION IV
GROWTH CAPABILITY

4.1 SCALING

The most important issue concerning the copper vapor laser is its capability to achieve high pulse energies at high average powers. In particular for this program it is the possibility of producing 50 millijoules or more per pulse at repetition rates greater than 200 Hz. This section reviews all of the pertinent experimental data to resolve this question. The conclusion can be drawn from the data that 50 millijoules or more is possible and could be obtained in the near future. No limitation in the physics of the lasing process precludes these pulse energies and the required electronic components can be acquired. The requirements for this system are given at the end of this section.

The design of a 50 millijoule system requires a clear understanding of the design parameters which govern the production of the pulse energy. For the design configurations discussed in this report, the parameters have been identified as:

a) laser tube input charge density;

b) its equivalent input specific energy density;

c) active lasing volume; and

d) copper atom number density.

Analysis of all of the data presented in the previous sections and in the appendices has permitted the present knowledge on growth capability to be summarized in figures provided in this section. These figures will present the specific and total pulse output energies as functions of the laser tube input charge density and active lasing volume. The specific energy density is equivalent to the first of these and the useable copper atom density is limited by metastable production.

For the data under consideration here, the input energy density is proportional to the input charge density and so the figures could just as easily be drawn as

specific output energy and energy per pulse as functions of input energy density. The reason behind this direct relationship stems from the fact that the peak voltage across all the discharge tubes was essentially the same. That is, at 1.0 kHz to 2.0 kHz, all the tubes broke down at between 12 and 13 KV and fell to zero in approximately 70 nsec. By multiplying the voltage across the tube times the current through it at each point in time and integrating, the input energy per pulse can be computed. When this is done, the result is a constant factor related to the break down voltage times the total input charge. Hence, the input energy density is proportional to the input charge density for all the tubes tested and the figures can be converted to show how the specific energy and pulse energy vary with the input energy density.

Figure 28 shows the maximum operating conditions achieved for all of the laser tubes investigated. Their specific output energy is displayed as a function of input charge density as measured into the laser tube. The tubes were only considered at a maximum operating condition for copper atom number density (temperature) when increases in the power supply output did not significantly increase laser output.

It is believed that the laser output was limited by the build-up of the lower laser state population. Experimental evidence for the onset of the limiting condition was the development of a "donut" shaped beam with a bright outer ring and a lower intensity center. The bright ring is interpreted as an active lasing volume where lower state depopulation is occurring during the inter-pulse period by copper atom collisions with the tube wall. The lower intensity center occurs when the inter-pulse period is too short to allow an adequate number of the excited copper atoms to migrate to the wall thereby building up the lower state population. The increased population produces laser radiation absorption and the occurrence of an apparent "donut-hole". The output power then "turns-over" or decreases as the discharge tube continues to heat up.

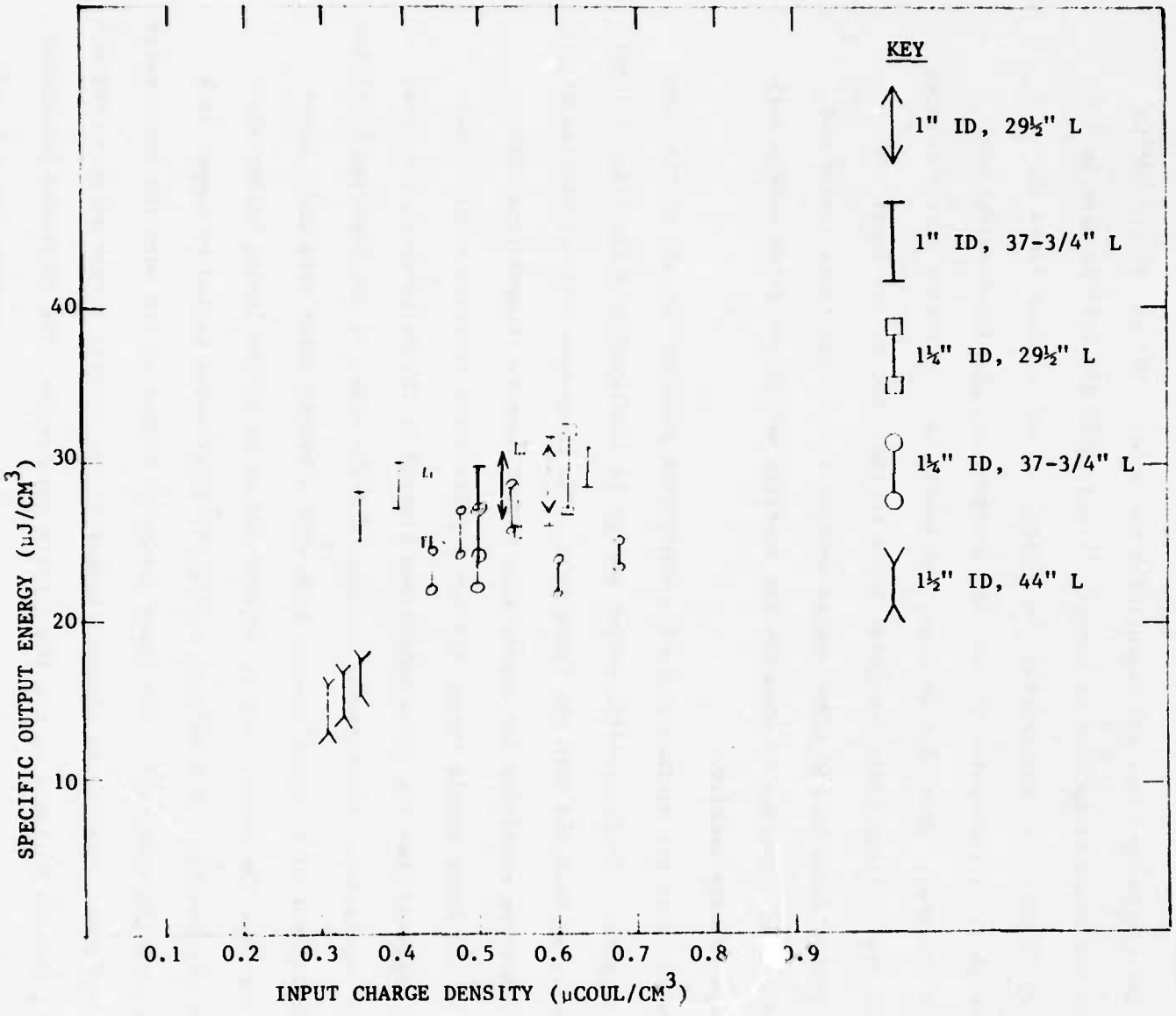

Figure 28. Specific Output Energy Operating Conditions for All Tubes Investigated

Increases in the discharge tube temperature and copper density leads to a growth of the "donut hole" and decrease ("turn over") in the output power. As might be expected, decrease in the time available for metastable diffusion to the walls, by increase of the repetition rate, causes formation of the "donut hole" and "turn over" to occur at a lower temperature. Similarly, increase of the discharge tube diameter increases the time required for a metastable to reach the wall and decreases the temperature at which turn over occurs.

The dependence of this turn over phenomenon upon input energy density and its behavior to either side of the optimum have not been discussed here due to a need for more reliable data. Clearly, more investigation is needed.

The above described experimental conditions were not observed with the 1½" ID laser tube at 1 kHz rates. This is apparent in Figure 28 in which all of the smaller tubes appear to reach an operating limit of 25 to 30 $\mu J/cm^3$ and at this limit are essentially independent of input charge (or energy) density. The best operating condition achievable for the 1½" ID tube was 12.5 to 17.5 $\mu J/cm^3$.

The operating state for the 1½" ID tube was limited by the availability of adequate electronic components and not limited by laser physics. This position is supported by Figure 22 and its related discussion in Section 3.4. The output was shown there to increase with peak current and the effectiveness of energy coupling into the laser tube. The availability of capacitors with higher voltage ratings and/or the use of more than one thyratron can be expected to permit higher peak currents and hence higher lasing specific energies in the 1½" ID tube.

The relative behavior of the tubes with respect to total output pulse energy is displayed in Figure 29. Again there is a strong suggestion the 1½" ID tube is in a different operating condition than the others. Most of the tubes show a small positive slope with increasing input charge density. The 1½" ID tube

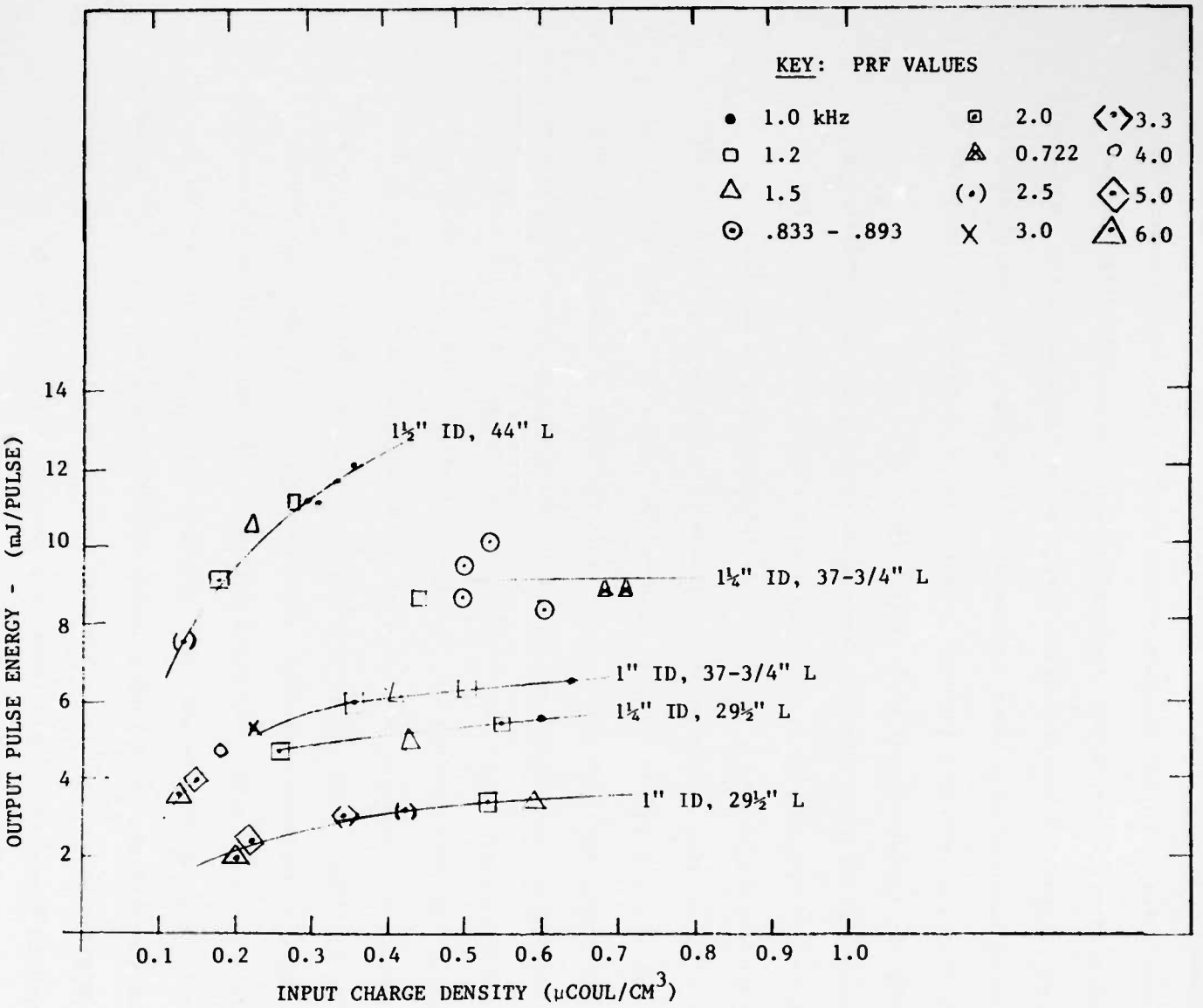

Figure 29. Total Output Pulse Energy Dependence on Input Charge Density

clearly has a greater dependence on input charge density and has not yet reached its peak output pulse energy. Figures 28 and 29 also both suggest that an input charge density greater than 0.4 μcoul/cm^3 is required at lower PRF values before the limiting condition is reached.

It is important to point out the natural separation of data based on tube dimensions as one considers total output energy as opposed to specific energy density. For specific energy density (Figure 28), the data are clustered and essentially independent of tube dimensions. The total output pulse energies (Figure 29), are dependent on tube dimensions. Figure 30 displays data from Figure 29 in a different format. An operating condition of 0.4 microcoulombs/cm^3 was selected, since data for all the tubes investigated either encompassed this condition or were very close to it. The experimentally derived total output pulse energy is observed to be dependent on the active volume of the laser. The data point deviating from a linear 45^o slope relationship is the 1½" ID tube which has not reached its optimal operating condition. If, after suitable optimization not completed on this program, this data point were to fall on the linear relationship, a specific energy density of 25.7 microjoules/cm^3 would be required. This energy density is consistent with the optimum conditions shown in Figure 28. All of the available data makes it reasonable to expect that the linear scaling will hold for the 1½" ID tube when proper optimization is completed.

How far beyond a 1½" ID tube with a 44" length will linear scaling continue to be valid is a very interesting question. If it is valid for a 1-3/4" ID tube with a 44" length, then a 25 mJ/pulse is possible. If it is valid for a 2" ID tube with a 44" length, then 32 mJ/pulse is possible. The physical limits to scaling will occur with:

a) tube diameter increasing to a size where quenching of the copper lower state at the side walls is no longer effective, and

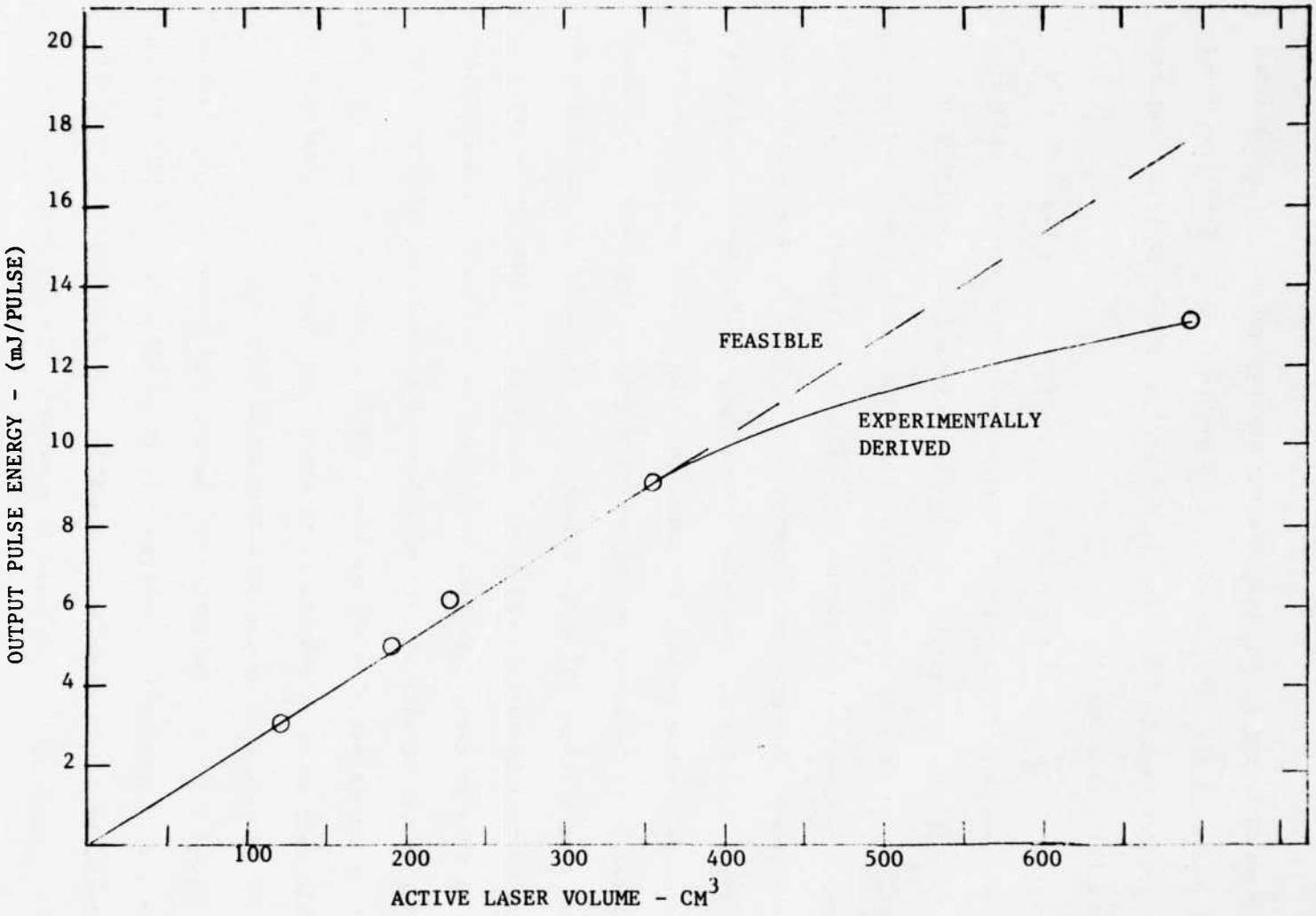

Figure 30. Total Output Pulse Energy Dependence on Active Laser Volume

b) tube length increasing to a size where the discharge becomes unstable and unsuitable for reliable lasing.

The dimensions where these physical limits set is cannot be predicted at this time. However, they are expected to be beyond a tube length of 2 meters since such lengths have been used at JPL in their copper halide laser program.

While operation of tubes at 25 to 30 microjoules/cm^3 has been achieved, increases in the specific energy are possible with improvements in the experiment configuration. Discussions in the early sections of this report indicated the use of 20^o off-vertical windows with an internal output coupler can produce a 10% improvement in performance. In addition, the laser reflecting mirror is known to have degraded during its lifetime; thereby reducing the laser output with its increased absorption. The combination of all these factors should permit a 15% improvement making 35 microjoules/cm^3 feasible. Thus it is reasonable to design a 50 millijoule per pulse device using a specific energy of 35 μjoules/cm^3 as a starting point.

To obtain 50 millijoules/pulse at 5105Å, the total pulse energy must be 70 millijoules. The use of two laser modules producing 35 millijoules per pulse would satisfy this requirement. Assuming a specific energy of 35 μjoules/cm^3, then a 1 liter active volume would produce the 35 millijoule pulse. Two of these lasers, either side by side or in a MOPA configuration, would produce 70 millijoules per pulse with 50 millijoules at 5105 nm.

A high confidence approach based on Figure 28 and anticipated improvements, can produce 35 μJ/cm^3 in a 1¼" ID discharge tube with a charge density of approximately 0.6×10^{-6} coulombs/cm^3. The demands on the power supply will be controlled by the laser operating efficiency. Figure 31 summarizes demonstrated efficiencies based on data in the appendix, for all of the tubes operated at the lower PRF values.

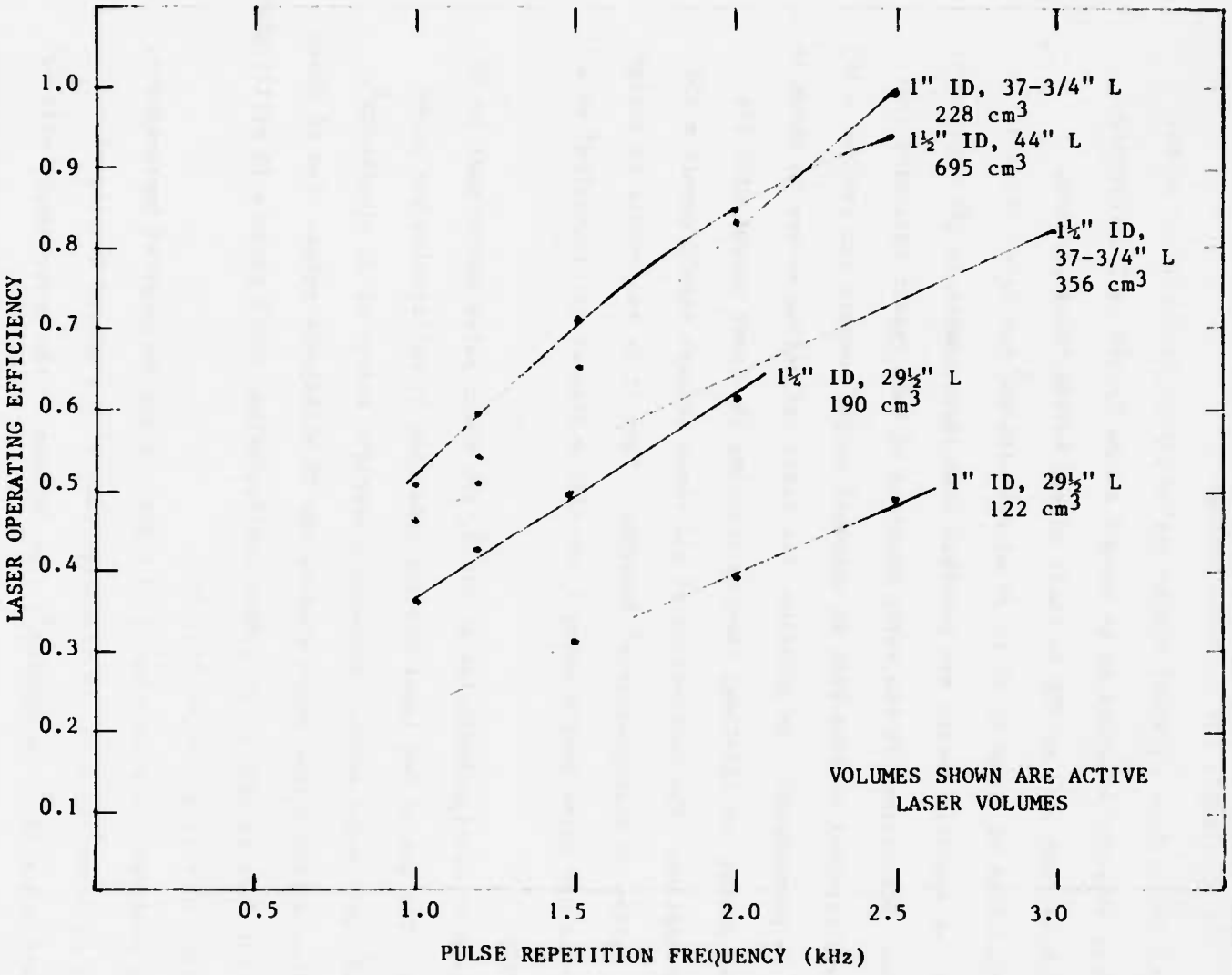

Figure 31. Laser Tube Operating Efficiencies (Output Power/Input Supply Power)

The achieved operating laser efficiency is approximately 0.5% for the 1½" ID tube at a PRF of 1.0 kHz. This implies a power supply input of 7 millijoules/cm^3 in each laser module to achieve the desired specific output energy of 35 μJ/cm^3. The equations below calculate the capacitance, voltage and peak currents that would be required from the above.

Charge Stored on Main Capacitor

$$Q = CV = 9\nu = 0.6 \times 10^{-6} \frac{coul}{cm^3} \times 1361\ cm^3 \tag{7}$$

$$CV = 8.2 \times 10^{-4}\ \text{coulombs}$$

Energy Stored on Main Capacitor

$$\tfrac{1}{2}CV^2 = \varepsilon\nu = 7 \times 10^{-3} \frac{joules}{cm^3} \times 1361\ cm^3 \tag{8}$$

$$\tfrac{1}{2}CV^2 = 9.5\ \text{joules}$$

Capacitance

$$C = 35\ nf \tag{9}$$

Voltage

$$V = 23\ KV \tag{10}$$

Peak Current

$$I_{max} = \frac{Q}{T} = \frac{8.2 \times 10^{-4}\ coul}{60 \times 10^{-9}\ sec} = 14{,}000\ amps \tag{11}$$

Laser Length

$$\text{Volume} = 1361\ cm^3 = \frac{\pi}{4}\left[1.25"\right]^2\left[2.54\right]^2 \times \ell \tag{12}$$

$$\ell = 172\ cm$$

Inductance

$$L = \frac{\mu_0}{4\pi} = \ell \left| n \frac{r_0}{r_2} = 4 \times 10^{-8} \right. \tag{13}$$

Pulse Width FWHM

$$\nu \frac{T}{4} = \frac{\pi \sqrt{LC}}{4} = 60\ nsec \tag{14}$$

Therefore, to produce the 35 millijoules per pulse laser module would require a main storage capacitor of 26 nf charged to 23 KV by a power supply capable of providing 7 KW average power. This would discharge into a 1000 cm^3 volume in a current pulse with FWHM of 60 nsec and hence a peak current of 14,000 amps. An ITT F-155 thyratron could handle these currents and voltages.

Using a 1¼" diameter discharge tube with an active length of 126 cm could thus be one way of producing a 1 liter volume. Subsequent experiments may indicate that 35 μjoules can also be obtained in a 1½" diameter tube and then the length would only be 87.6 cm. Even larger diameter tubes operating at less than 35 $\mu J/cm^3$ could produce a 35 millijoule module further reducing the overall system's length.

Of course, the use of a larger diameter laser tube could lead to a single module producing the full 70 mJ pulse. Since this would involve extrapolating the curve on Figure 30 considerably beyond the available data, this alternative cannot be considered one of as high confidence as that of the two module, 1¼" ID tube, approach. Nonetheless, a 1-3/4" ID tube, 190 cm long could have an active volume of 2184 cm^3 and produce the desired 70 mJ with 32 $\mu J/cm^3$ specific energy. The corresponding circuit requirements determined using equations (7) - (11) are:

$$C = 57 \text{ nf} \qquad V = 23 \text{ KV} \qquad I_{max} = 16 \times 10^4$$

These again are practical values.

It is important to state then that no limit in energy per pulse has yet been reached and that production of 50 millijoule pulses at 5105Å can be accomplished in the very near future.

4.2 CONCEPTUAL BRASSBOARD DESIGN

Sufficient progress was made during the course of the program to permit the generation of a conceptual brassboard design capable of greater than 50 mJ/pulse and suitable for Navy field applications. An important feature of the laboratory results was the predictability of laser performance as design parameters were modified. In most cases, the impact on performance was either predicted prior to the tests or readily modelled using first order principles once the results were obtained. The test runs with apparently anomalous behavior during laser operations were usually traceable by post-operation investigations to degraded or failed

components. An adequate confidence level was developed, therefore, in the ability to quantitatively specify design parameters (e.g., tube length, number of radiation shield layers, amount of copper, etc.) and build a laser with predictable performance properties. The extent to which this design scaling is valid beyond the demonstrated performance range is yet to be explored.

The basic laser to be used in this brassboard design was described in the last section. The high confidence approach using two 1¼" ID laser tube modules was chosen.

The component functions for the brassboard design are a direct carryover from the present laboratory hardware. The functional block diagram is shown in Figure 32. Each of the laser components exist in their laboratory form and have many hours of reliable operation. The exceptions are the "power conditioners" and the "controllers". The former are not required with the availability of standard 120 VAC in the laboratory. The latter are presently accomplished by manual operation.

The power supply controller functions are to:

a) control laser heat-up sequence for gradual or rapid heating modes,

b) establish a desired output power operating level,

c) maintain long term output power stability via a signal feedback network.

The pulse network controller functions are to:

a) establish optimum pulse conditions (width and amplitude) for operation at a specified pulse repetition rate, and

b) provide the control point for pulse modulation schemes (e.g., for communication applications) via electronic input commands.

The circuits for the brassboard design are provided in Figures 33 to 35 for the resonant charging circuit, pulse forming network, thyratron bias circuit, and pulse network controller (manual version). The functional block diagram for the pulse network controller is given in Figure 34 and the associated circuits in Figure 35.

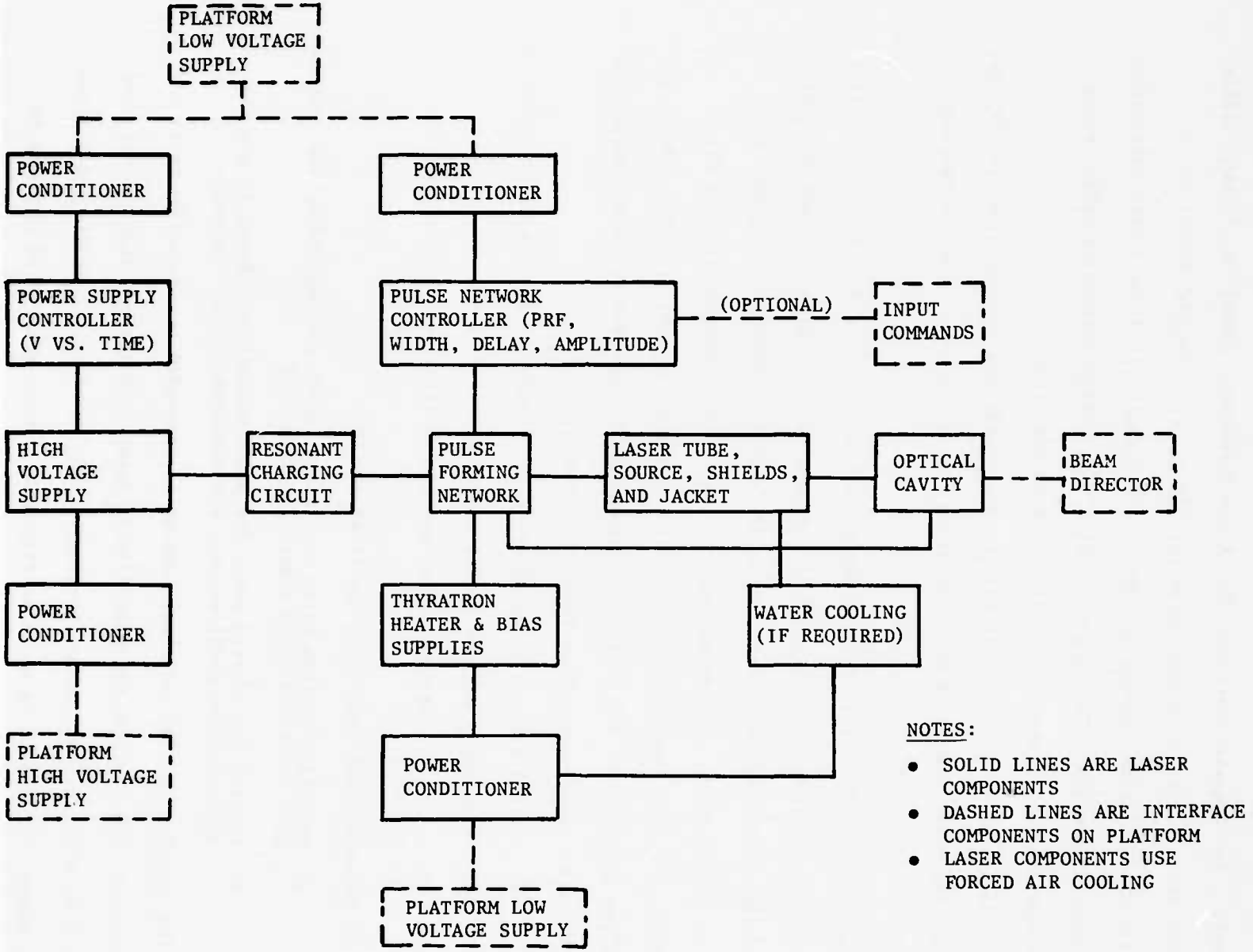

Figure 32. Laser Brassboard Functional Block Diagram

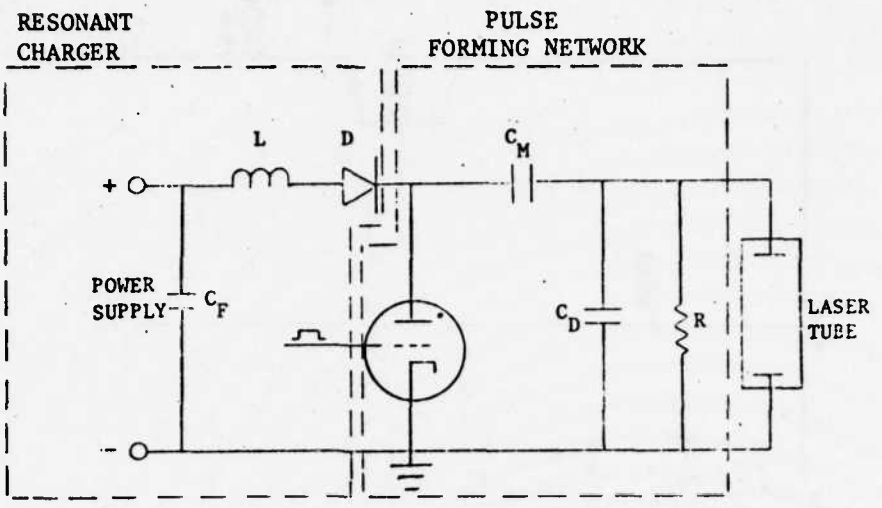

TYPICAL CIRCUIT PARAMETERS

L = 300 mH D = 6, 8 kV diodes in a series/parallel combination for 24 kV @ 1A

C_M = 26 nF R = 150 Ω, 200 W

C_D = 10 nF C_F = 3 μF

Figure 33. Pulse Forming Network With Resonant Charging

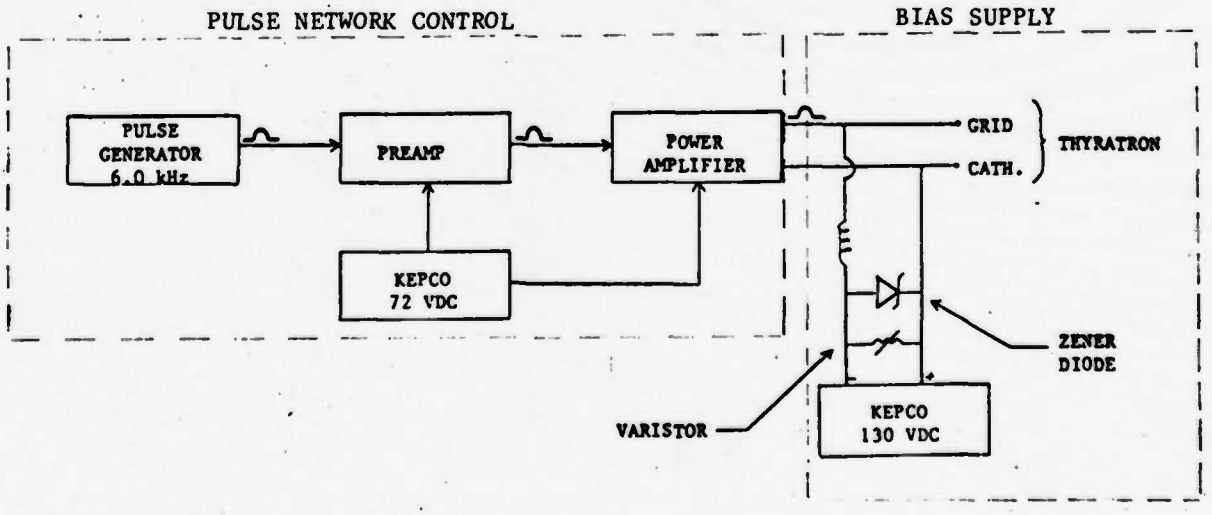

Figure 34. Pulse Network Control and Bias Supply

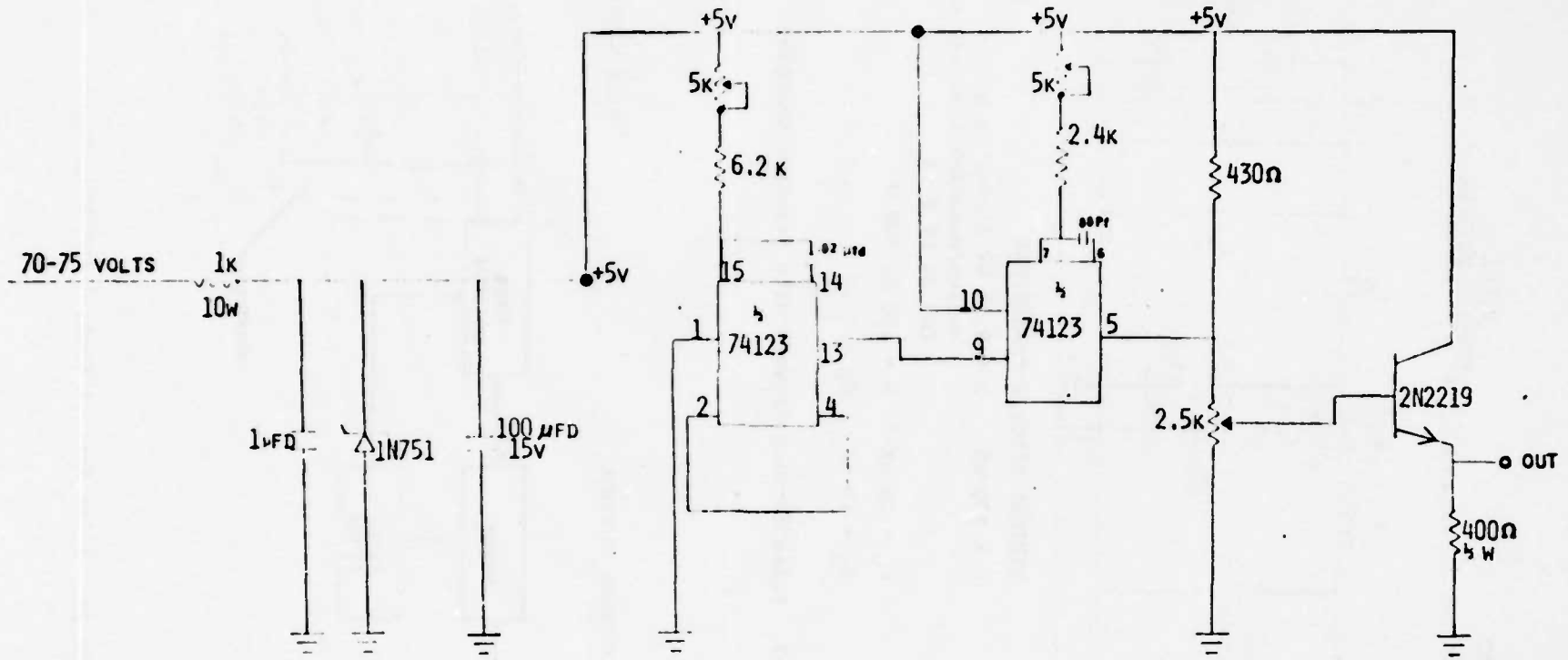

Figure 15A. Trigger Pulse Generator For Pulse Network Controller

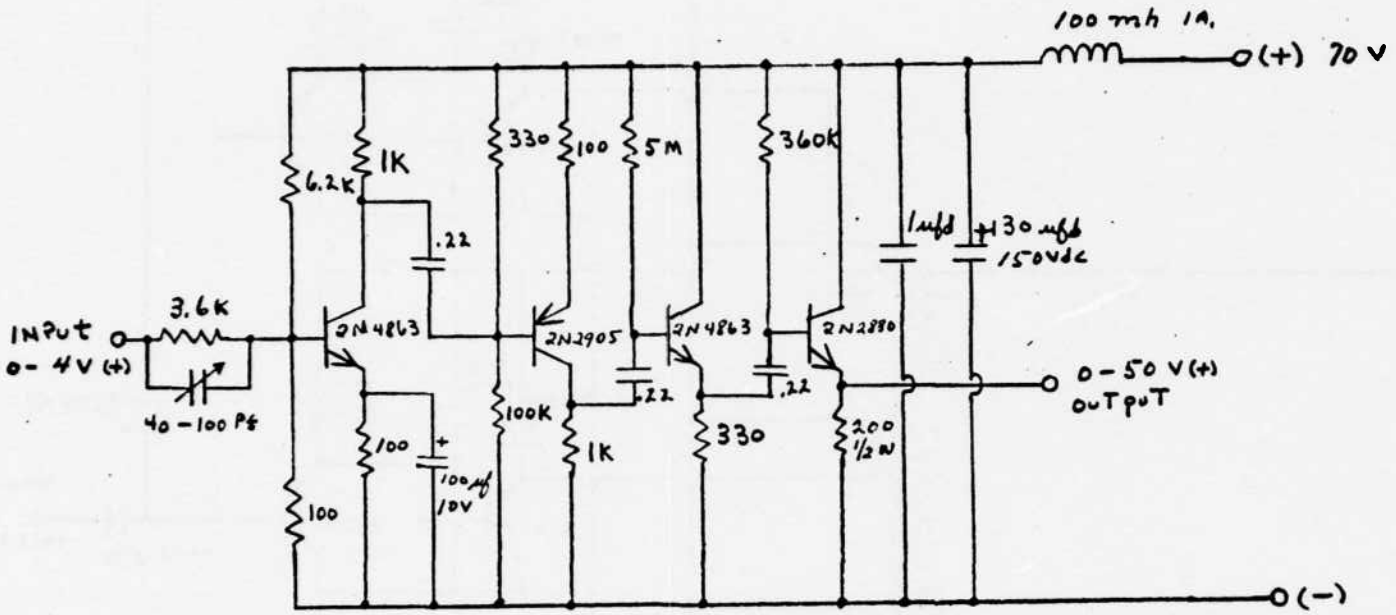

Figure 35B. Trigger Pulse Voltage Amplifier (Preamp) For Pulse Network Controller

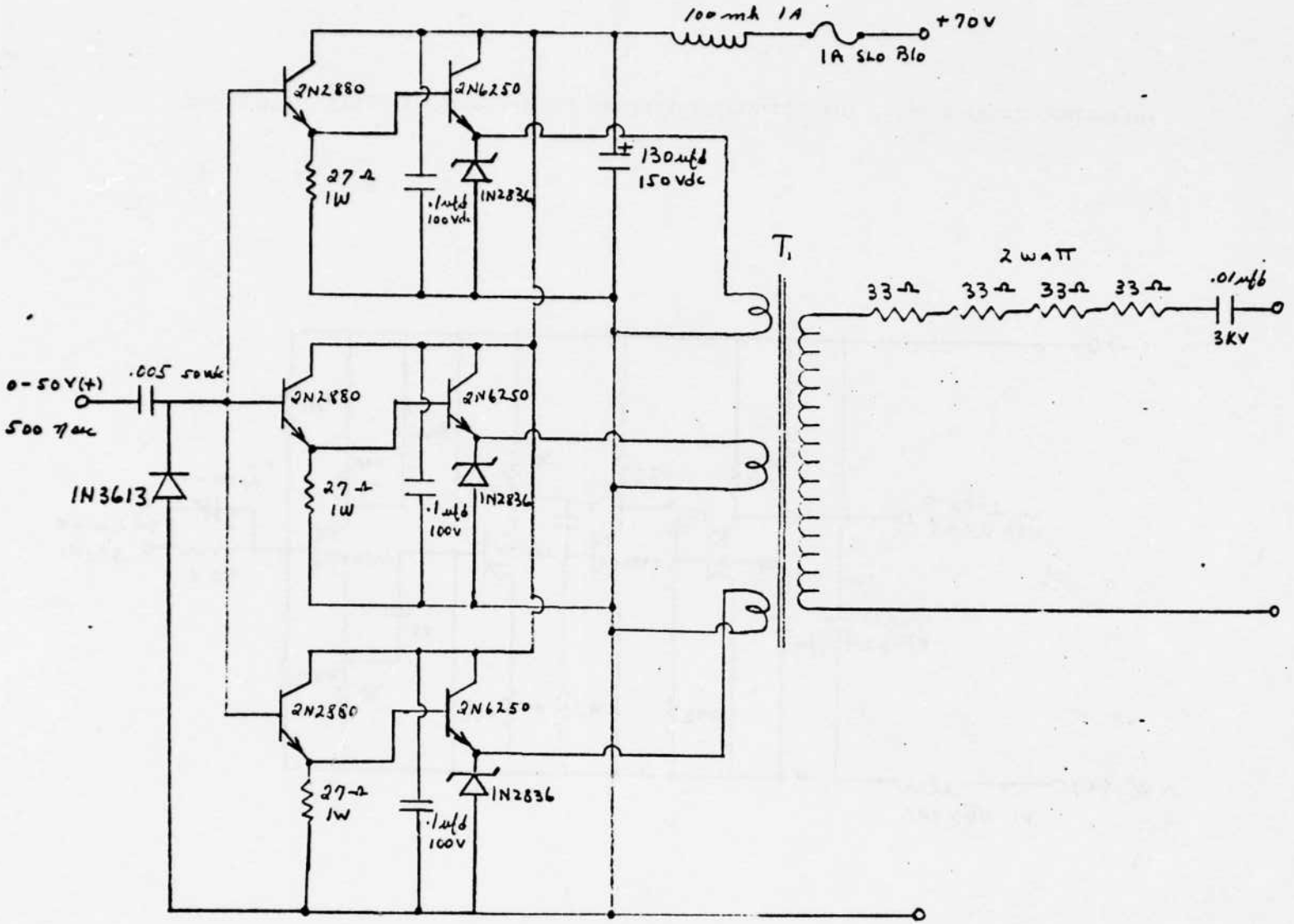

Figure 35C. Trigger Pulse Power Amplifier For Pulse Network Controller

The details of the power conditioners have been omitted at this time because of their close dependence on the specific capabilities of various operating naval platforms. The conditioners provide the interface compatibility between the laser and the operating platform power capabilities.

An important feature of any brassboard design is the configuration of the system into a minimal weight and volume to evaluate fieldability. A practical configuration is given in Figure 36. The selection of the components shown has been based on the design requirements given in Section 4.1. All the electronics are in their reduced form. The laser shows anticipated advances in design over the one described in Sections 2.3.3 and 3.1. The advances include:

a) no water cooling;

b) sealed laser without a vacuum system;

c) output windows at a 20^{o} angle to the vertical to optimize the output of both polarization components; and

d) increased vacuum jacket diameter to easily incorporate sufficient shielding layers for high millijoule per pulse operation.

The estimated volumes are:

7.0 KW High Voltage Power Supply	3.0 ft^3
Resonance Charging Circuit	1.0 ft^3
Laser & Bias, Heater & Pulse Electronics	$\lesssim$5.0 ft^3
All Else (Fans, Conditioners, Controllers)	$\sim$1.0 ft^3

The associated weight estimates are:

7.0 KW Power Supply	140 lbs.
Resonance Charging Circuit	50 lbs.
Laser & All Other Electronics	60 lbs.
All Else (Fans, Support Structures, etc.)	60 lbs.

These estimated values can be accommodated by a broad range of existing airborne and naval platforms. Further reductions in weight and volume can be expected once detailed engineering activity is initiated.

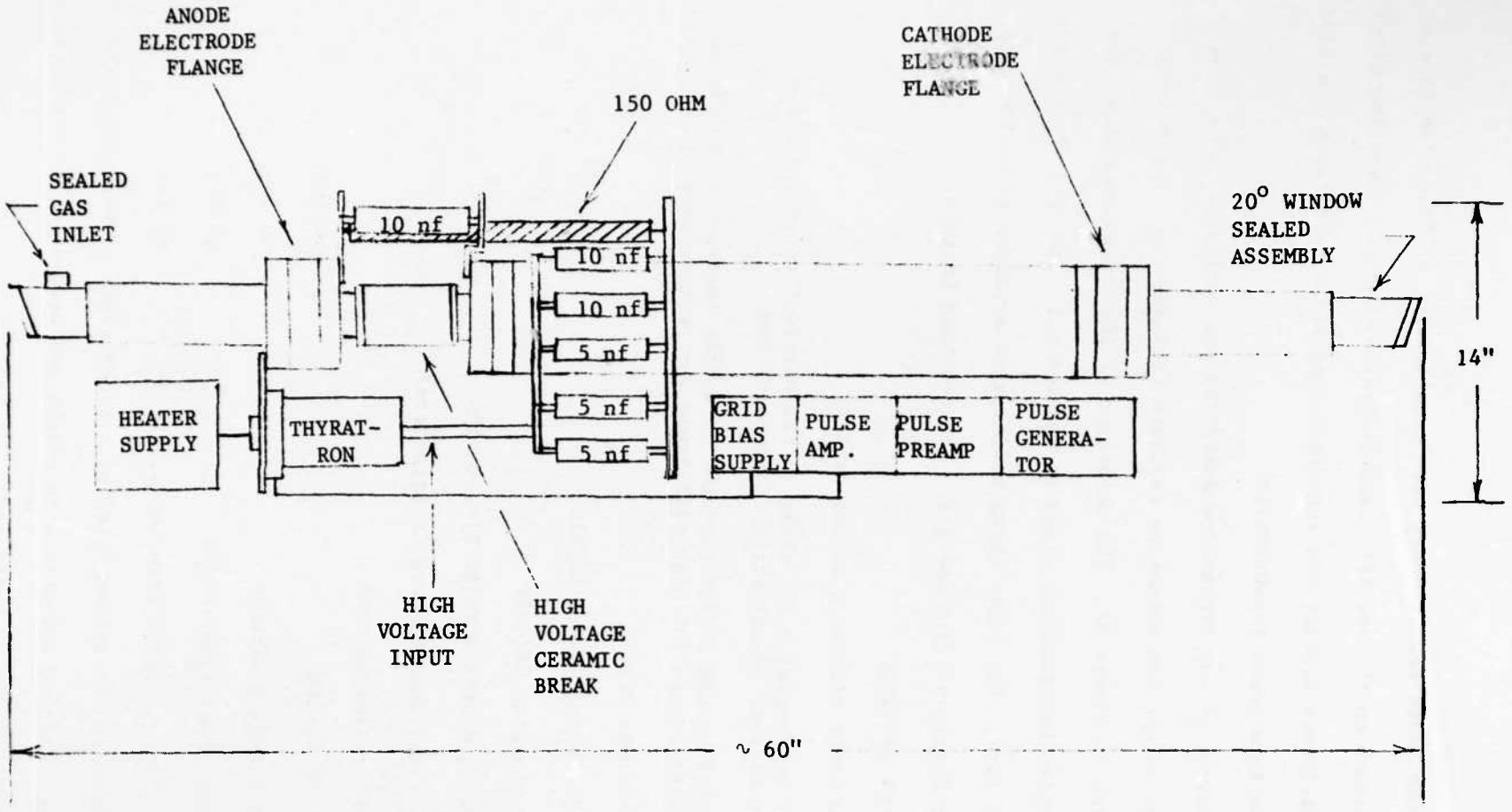

NOTE: NOT SHOWN ARE THE

- HIGH VOLTAGE SUPPLY OCCUPYING 3.0 FT^3
- RESONANCE CHARGING CIRCUIT OCCUPYING 1.0 FT^3

Figure 36. CVL Conceptual Brassboard Configuration

The transition from laboratory apparatus to brassboard hardware is anticipated to be feasible with no insurmountable engineering obstacles. Many components are similar to modules previously designed by G.E. Aircraft Equipment Systems Department for aircraft apparatus. The areas identifiable at this time requiring brassboard engineering design and demonstration are:

- Miniaturization and volume reduction of the pulse forming network, resonance charging network, thyratron heaters and bias circuits, and primary DC high power supply (if power not available from operating platform)
- Elimination of vacuum pumping system
- Elimination or significant reduction of the water cooling system and its, at least, partial replacement with forced air cooling
- Low maintenance levels for the optical cavity with regard to alignment and transmission/reflection values
- Ease of laser tube replacement
- Operation times between copper or laser tube replacement in excess of 100 hours of lasing.

Several of these problems are currently being addressed. Techniques for making a sealed off laser tube not requiring a vacuum system are being evaluated under a G.E. IR&D program. Techniques for recirculating copper so that operation might be maintained for 400 hours is being studied with ERDA support.

The incorporation of these design features into a brassboard will produce an operating laser with characteristics closely akin to an advanced engineering model. Engineering application, packaging, scale-up design, and cost studies could then be reliably performed for a spectrum of potential naval applications.

SECTION V

CONCLUSIONS AND RECOMMENDATIONS

5.1 CONCLUSIONS

This program has developed a discharge heated pure-copper vapor laser with output characteristics capable of satisfying several Naval underwater transmission applications. The laser has produced an output of 12.12 millijoules per pulse at 1.0 kilohertz. This performance represents a factor of 7 improvement in the technology available prior to this program. The performance parameters have sufficient growth capability to make a brassboard 50 millijoule laser system feasible and practical. No physical limitations have been found to impede the production of the brassboard system in the near future. Packaging of the system is compatible with a broad range of Navy sea and airborne platforms.

The key to the growth capability is the linear scalability of output pulse energy with active lasing volume. The scaling has been found to be valid for all the tube sizes investigated in this program provided the input charge density exceeds 0.4 microcoulombs/cm^3 and the tubes are in their optimal specific energy regime of 25 - 30 microjoules/cm^3. The limits in tube diameter and length for which linear volume scaling is no longer valid have not been found. Design improvements which have been demonstrated in the program and are readily implementable can raise the tube specific energy to 35 microjoules/cm^3. These include: 20^o off vertical windows, internal output coupler, and a high quality total reflection cavity mirror. At this 35 $\mu J/cm^3$ level, a two tube laser system with 2000 cm^3 of total active lasing volume will produce 50 millijoules per pulse at the 5105Å line.

Transition to a brassboard laser is expected to be a straightforward engineering process. All of the key electronic circuits have been tested and found to give long life reliable performance. Miniaturization of the components presents no obvious problems. The laser design configuration is inherently rugged and amenable

to compact packaging. The implementation of a sealed off laser tube eliminating the need for a vacuum system and with copper recirculation is on the near horizon. The electronic components (particularly thyratrons, capacitors, and power supplies) for 50 mJ/pulse operation are in existence. The laser conceptual brassboard design down to the component level, therefore, can be and has been defined in this program.

5.2 RECOMMENDATIONS

The improvements achieved during the past year in the performance of self-heated copper vapor lasers and their demonstrated capability for growth to even higher pulse energies have produced a good technical basis for continued development. The development and demonstration of a 50 millijoule per pulse brassboard laser system is, therefore, recommended. The objectives for the recommended activity should be:

a) obtain experimental data to better characterize design scalibility and limits;

b) produce 50 millijoules per pulse at 5105Å using a brassboard laser system;

c) evaluate field performance capability with regard to signal transmission, maintainability, reliability and operating lifetime between servicing.

Specific technical recommendations supporting the performance objectives are:

a) increase the output pulse energy in a laser module by increasing tube inside diameters above 1½", increasing tube lengths beyond 44", increasing input specific energies in tube with 1¼" and greater ID tubes using thyratrons in parallel, increasing capacitor voltages, and optimizing window design for improved output coupling.

b) achieve at least 35 millijoules per pulse using a 1¼" ID tube with a 126 cm length since this tube provides at the present time the highest confidence path to the desired pulse energies.

c) establish improvements in output pulse energies achievable by lower PRF and higher copper densities in each of the tubes to be evaluated, particularly through control of lower laser state population.

d) increase pulse peak powers by incorporating the identified shielding techniques for decreasing circuit inductance.

e) operate and synchronize two lasers in parallel to achieve 50 mJ/pulse at 5105Å, test reliability and establish losses from integrating optics.

f) demonstrate sealed laser tube performance with copper recirculation at desired pulse energies.

g) miniaturize and operate associated electronic components.

h) assembly and test brassboard over a range of operating conditions.

REFERENCES

1. R. S. Anderson, et al, "Discharge-Heated Copper Vapor Laser, MOPA Operation," Final Report AFAL-TR-76-93, Air Force Avionics Laboratory, (1976).

2. B. G. Bricks, et al, "Copper Vapor Laser," AFWL-TR-75-197, Air Force Weapons Laboratory, (1975).

3. W. T. Walter, N. Solimene, M. Piltch and G. Gould, "Efficient Pulsed Gas Discharge Lasers," IEEE J. Quan. Elec. QE-2, 474, (1966).

4. W. T. Walter, "40kW Pulsed Copper Laser," Bull. Am. Phys. Soc. 12, 90 (1967).

5. W. T. Walter, private communication.

6. R. J. L. Chimenti, "The Copper Vapor Laser," Ph.D. Thesis, Polytechnic Institute of Brooklyn, June 1972. (unpublished)

7. J. F. Asmus and N. K. Moncur, "Pulse Broadening in a MHD Copper Vapor Laser," App. Phys. Lett. 13, 384 (1968).

8. G. R. Russell, N. M. Nerheim and T. R. Pivirotto, "Supersonic Electrical-Discharge Copper Vapor Laser," App. Phys. Lett. 21, 565 (1972).

9. C. M. Ferrar, "Copper-Vapor Laser with Closed-Cycle Transverse Vapor Flow," IEEE J. Quan. Elec. QE-9, 856 (1973).

10. T. W. Karras, R. S. Anderson, B. G. Bricks, T. E. Buczacki and L. W. Springer, "Copper Vapor Generator", AFWL-TR-73-133, Air Force Weapons Laboratory, Kirtland AFB, NM (1973).

11. C. J. Chen, N. M. Nerheim and G. R. Russell, "Double-Discharge Copper Vapor Laser with Copper Chloride as a Lasant," App. Phys. Lett. 23, 514 (1973).

12. C. J. Chen and G. R. Russell, "High-Efficiency Multiply Pulsed Copper Vapor Laser Utilizing Copper Chloride as a Lasant," App. Phys. Lett. 26, 504 (1975).

13. I. Liberman, R. V. Babcock, C. S. Liu, T. V. George and L. A. Weaver, "High-Repetition-Rate Copper Iodide Laser," App. Phys. Lett. 25, 334 (1974).

14. A. A. Isaev, M. A. Kazaryan and G. G. Petrash, "Effective Pulsed Copper-Vapor Laser with High Average Power Generation," JETP Lett. 16, 27 (1972).

15. T. S. Fahlen, "Hollow-Cathode Copper-Vapor Laser," J. Appl. Phys. 45, 4132 (1974).

16. R. S. Anderson, L. W. Springer, B. G. Bricks and T. W. Karras, "A Discharge-Heated Copper Vapor Laser," IEEE J. Quan. Elec. QE-11, 173 (1975).

17. A. A. Isaev, M. A. Kazaryan and G. G. Petrash, "Copper Vapor Laser with a Repetition Frequency of 10 kHz," Opt. Spectros. 35, 307 (1973).

18. L. A. Weaver, C. S. Liu and E. W. Sucov, "Superradiant Emission at 5106, 5700 and 5782 Å in Pulsed Copper Iodide Discharges," IEEE J. Quan. Elec. QE-10, 140 (1974).

19. W. E. Austin, "100kHz Quenching Spark Gaps," Laser Focus 11, 79 (1975).

20. R. S. L. Chimenti, "Heat-Pipe Copper Vapor Laser," Final Report to Contract N0014-73-C-0317, 1974.

21. W. T. Walter, Polytechnical Institute of New York, Joint Services Technology Advisory Report No. R452-41-76 (1976).

22. G. R. Russell, JPL, private communication.

23. I. S. Alexandrov, et al, Soviet Journal of Quantum Electronics, Vol. 5, No. 9.

24. R. S. Anderson, et al, Air Force Avionics Lab Contract F33615-76-C-1137.

25. R. S. Anderson, et al, ERDA Lawrence Livermore Laboratory Contract 5949703.

26. R. W. Getzinger, N. R. Greiner, K. D. Ware, J. P. Carpenter and R. G. Wenzel, IEEE J. Quan. Elec. QE-12, 556, (1976).

APPENDIX A

PHYSICAL CHARACTERISTICS OF LASER TUBE ASSEMBLIES

A range of laser tube physical characteristics was evaluated during the program. The variations in characteristics had a significant impact and, therefore, had to be taken into account in the assessment of laser performance. The most important characteristics are discharge length, area and volume, active lasing volume, radiation shield configuration, and copper source locations. These items have been discussed in the body of the report and will not be repeated here.

Table A-1 provides the detailed and quantitative description of the physical characteristics for those laser tubes having the best performance and selected for evaluation. A series of experiments were generally required to establish the conditions for optimal performance. The tube diameters and total lengths shown in the table are accurate to within 5%. The uncertainty in tube diameter arises from its natural taper from one end to the other which is an artifact of the fabrication process. The diameters shown are average values. The uncertainty in the total effective electrical length is caused by observed variations in the discharge behavior during tube operation.

The calculated flange to flange volume has been used to define the charge and energy density into the tube. The active lasing volume determined by the tube's "hot" zone (see Section 3.4) has been used to define the output specific energy in $\mu J/cm^3$.

The radiation shield configurations described in the table were the ones producing an acceptable tube temperature and operating power efficiency. Variations in the materials used for the shields and spacers are evidence of the investigation to find an economical design with long operating life potential and ease of assembly. The best configuration in these respects found in the program involve the use of

Table A-1. Laser Tube Physical Characteristics

Tube Dimensions		Tube Volume		Radiation Shield Configurations		
Inside Diameter (m)	Length* (in)	Flange to Flange* (cm^3)	Lasing Active** (cm^3)	Shield Material Type	Number of Layers	Shield Spacer Material
1.0	29.5	379	148-122	Molybdenum Foil	11	Alumina Powder
1.0	37.75	486	254-228	Molybdenum Foil in Stainless Steel Tube	8	Tungsten Wire
1.25	29.5	592	230-190	Molybdenum Foil	17½	Tungsten Wire
				Molybdenum Taper on Cathode	5	Tungsten Wire
1.25	37.75	757	396-356	Molybdenum Foil	10	Alumina Powder
				Nickel Foil	4	Alumina Powder
				Molybdenum Foil	2	Tungsten Wire
				Molybdenum Tapers on Electrodes Tapers	2½	Tungsten Wire
1.5	44	1274	753-695	Molybdenum Foil	8	Saffil
				Nickel Foil	16	Saffil
				Molybdenum Tapers on Electrodes	2	Saffil
1.5	46	1331	868-752	Molybdenum Foil	5	Saffil
				Molybdenum Foil	8	Tungsten Wire
				Molybdenum Tapers on Electrodes	4	Tungsten Wire

* Includes alumina tube length plus electrode lengths into flanges

** Governed by copper deposition sites which define "hot" zone, see Section 3.4

molybdenium foil for the innermost layers, nickel foil for the outer layers, and Saffil spacer material.

APPENDIX B

LASER TUBE PERFORMANCE DATA

The tubes investigated most thoroughly in the program ranged in tube inside diameters from 1.0" to 1.5" and lengths from 26" to 44". They were operated under a variety of electrical and thermal conditions to establish performance trends and optimal output capability. The trends and optimal laser capabilities have been discussed in the body of the report. This appendix provides the detailed experimental data for those tubes selected for evaluation and operating at the best conditions.

The data tables are given; one for each tube diameter evaluated. The physical characteristics for these tubes have been described in Appendix A. The connection between the appendices is keyed by the tube dimensions of inside diameter and total length (includes electrode length into flanges).

The input and output data shown are for the tubes at their optimal performance levels. These levels were determined by a systematic variation in input parameters (e.g., capacitor ratios, voltage/current, gas pressure, etc.) until optimal output conditions (e.g., total output power, energy output/pulse, etc.) were established. The best performance achievable was at times not limited by the laser tube capability but rather by input parameter limitations such as capacitor voltage ratings, power supply current limits, thyratron current capability. This is particularly applicable to the tubes with 1.5" diameters and possibly those with 1.25" diameters. The data given in Tables B-1 to B-3 are for the best achievable conditions with available hardware.

The input charge densities are calculated using the total tube (flange to flange) volumes given in Table A-1. The output specific energies are calculated using the active lasing volumes from Table A-1. The output pulse energies are

Table 8-1. Laser Tube Performance Data - 1.0" ID

Tube Dimensions		Laser Tube Inputs						Laser Outputs		
Inside Diameter (in)	Length (in)	PRF (kHz)	Capacitor Ratio (nf/nf)	Supply Voltage (kV)	Supply Current (amps)	Supply Power (kW)	Charge Density ($\mu coul/cm^3$)	Total Power (W)	Specific Energy ($\mu J/cm^3$)	Pulse Energy (mJ)
1.0	29.5	1.46	13.0/2.5	4.9	328	1606	0.59	5.2	26.2/31.7	3.56
		2.0	13.0/2.5	4.5	408	1838	0.53	7.0	26.0/31.2	3.50
		2.5	11.5/2.5	4.0	400	1600	0.42	7.9	23.4/28.2	3.15
		3.3	9.0/2.5	3.9	416	1622	0.33	8.3	17.1/20.1	2.52
		5.0	6.0/2.5	4.0	400	1600	0.21	10.7	14.5/17.5	2.13
		6.0	6.0/2.5	3.7	456	1687	0.20	12.1	13.7/16.6	2.02
1.0	37.75	1.0	22.0/2	4.56	312	1422	0.64	6.6	28.1/31.2	6.56
		1.2	20.2/2	4.87	294	1389	0.50	7.6	27.0/30.0	6.3
		1.5	17.0/2	4.62	310	1433	0.40	9.4	27.0/29.7	6.25
		2.0	15.0/2	4.21	341	1434	0.35	11.9	25.2/28.1	5.97
		2.5	12.0/2	4.35	331	1440	0.27	14.2	24.3/24.8	5.68
		3.0	9.0/2	4.7	300	1411	0.21	16.1	21.0/23.4	5.35
		4.0	9.0/2	4.15	342	1422	0.18	18.2	17.9/19.8	4.54
		5.0	6.0/2	4.41	331	1457	0.14	20.0	15.7/17.4	4.0
		6.0	6.0/2	4.1	3756	1464	0.12	21.6	14.1/15.7	3.6

Table B-2. Laser Tube Performance Data - 1.25" ID

Tube Dimensions		Laser Tube Inputs						Laser Outputs		
Inside Diameter (in)	Length (in)	PRF (kHz)	Capacitor Ratio (nf/nf)	Supply Voltage (kV)	Supply Current (amps)	Supply Power (kW)	Charge Density ($\mu coul/cm^3$)	Total Power (W)	Specific Energy ($\mu J/cm^3$)	Pulse Energy (mJ)
1.25	29.5	1.0	20/2	5.4	288	1555	0.60	5.6	26.5/32.1	5.6
		1.2	20/2	4.8	318	1528	0.55	6.5	25.6/30.9	5.4
		1.5	15/2	5.0	306	1528	0.43	7.7	24.3/29.4	5.13
		1.6	15/2	4.81	319	1537	0.34	7.5	20.4/24.8	4.71
		2.0	15/2	4.29	351	1505	0.25	8.4	19.9/24.1	4.21
1.25	37.75	0.722	25/5	5.5	370	2035	0.68	6.5	23.0/25.2	8.98
		0.833	20/5	6.0	338	2048	0.54	8.5	25.7/28.6	10.19
		0.893	20/5	5.8	342	1983	0.51	8.6	24.3/27.0	9.65
		1.0	20/5	5.55	370	2053	0.49	9.6	24.2/26.9	9.6
		1.2	20/5	5.19	400	2076	0.44	10.5	22.1/24.6	8.76

Table B-3. Laser Tube Performance Data - 1.5" ID

Tube Dimensions		Laser Tube Inputs						Laser Outputs		
Inside Diameter (in)	Length (in)	PRF (kHz)	Capacitor Ratio (nf/nf)	Supply Voltage (kV)	Supply Current (amps)	Supply Power (kW)	Charge Density ($\mu coul/cm^3$)	Total Power (W)	Specific Energy ($\mu J/cm^3$)	Pulse Energy (mJ)
1.5	44.0	0.862	20/9	7.0	410	2880	0.26	10.4	14.3/16.7	12.1
		0.893	20/9	6.6	395	2607	0.35	10.6		11.84
		1.0	20/9	6.5	450	2925	0.35	12.1	14.9/17.4	12.1
		1.0	20/11	6.3	420	2646	0.33	11.6	14.1/16.7	11.64
		1.0	20/6	6.3	395	2489	0.31	11.3	13.7/16.0	11.30
1.5	46.0	1.0	20/5	5.52	397	2190	0.30	11.2	12.8/14.8	11.15
		1.2	20/5	5.9	438	2229	0.27	13.4	12.9/14.9	11.2
		1.5	10/5	5.2	440	2288	0.22	16.3	12.5/14.4	10.85
		2.0	15/5	4.3	482	2073	0.18	17.6	10.1/11.7	8.8
		2.5	10/5	4.86	422	2051	0.13	19.3	8.9/10.2	7.7
		3.0	10/5	4.38	470	2059	0.12	20.1	7.7/8.9	6.7

AD-A047 197 GENERAL ELECTRIC CO PHILADELPHIA PA SPACE DIV F/G 20/5
LOW REPETITION RATE COPPER VAPOR LASER.(U)
SEP 77 R S ANDERSON, R J HOMSEY, T W KARRAS N00014-76-C-0975

UNCLASSIFIED NL

2 OF 2
AD
A047197

END
DATE
FILMED
1-78
DDC

derived from the measured output powers and laser pulse rate frequencies. All other parameters in the tables are directly measured as described in Section 3.1.

APPENDIX C

POWER DISTRIBUTION IN LASER ASSEMBLY

There exists a number of components between the output of the power supply and the input to the laser tube which are potential sites for needless power losses. These sites contribute directly to undesirable reductions in laser efficiency and output pulse energies. An effort was made during the program to identify and characterize these sites. This appendix provides the detailed experimental results of the effort.

A brief analysis of the laser assembly led to the identification of four candidate sites for undesirable power dissipation. They are the thyratron, the two window assemblies, and the outer jacket of the vacuum assembly.

The water cooling system used in the laser experiments provided a very convenient and practical scheme for measuring by calorimetric means the power dissipation at the first three of these sites. Losses in the outer jacket of the tube's vacuum assembly were not easily measured. These losses were, therefore, included as part of the power into the tube assembly which includes the alumina tube, its electrodes, the radiation shields, the ceramic break, and the outer vacuum jacket. Power losses were determined by the equation

$$\frac{dQ}{dt} = \frac{dm}{dt} C \Delta T$$

where $\frac{dm}{dt}$ is the water flow rate at each site, C is the specific heat of water, and ΔT is the change in water temperature caused by passage through the site.

The experimental results for the tubes studies are given in Table C-1. In addition to absolute power losses, at each site, the percentage losses relative to the power supply output are calculated. The study was not complete and more activity is required before a thorough understanding of power loss distribution and its mechanisms can be developed. Some preliminary conclusions are:

Table C-1. Power Distribution In Laser Assembly

Tube Dimensions		Laser PRF (kHz)	Supply Input Power (kW)	Entering Water Temperature (°C)	Laser Component	Cooling Water Temperature Change (°C)	Water Flow Rate (mℓ/sec)	Power Deposition (W)	Percent Total Power (%)
Inside Diameter (in)	Length (in)								
1.25	37.75	1.54	1349 (lasing)	7.5	Thyratron	3.5	11.1	162	12.0
					Anode Assembly	0.5	12.5	26	1.9
					Cathode Assembly	1.5	13.3	84	6.2
					Tube Assembly	-	-	1077	79.9
		1.2	1360	7.5	Thyratron	4.5	11.1	209	15.4
					Anode Assembly	1.5	12.5	108	7.9
					Cathode Assembly	2.0	13.3	111	8.2
					Tube Assembly	-	-	932	68.5
		1.2	1528	7.5	Thyratron	6.5	11.1	302	19.8
					Anode Assembly	2.5	12.5	139	9.1
					Cathode Assembly	2.5	13.3	130	8.5
					Tube Assembly	-	-	957	62.6
		1.2	1755	7.5	Thyratron	7.0	11.8	345	19.7
					Anode Assembly	2.5	12.5	130	7.4
					Cathode Assembly	3.5	14.3	209	11.9
					Tube Assembly	-	-	1071	61.0
		1.2	1809	7.5	Thyratron	7.0	11.8	345	19.1
					Anode Assembly	2.5	12.5	131	7.2
					Cathode Assembly	3.0	14.3	180	10.0
					Tube Assembly	-	-	1153	63.7
		1.0	1909	7.5	Thyratron	8.5	11.8	418	21.9
					Anode Assembly	3.5	12.5	183	9.6
					Cathode Assembly	3.5	14.3	209	10.9
					Tube Assembly	-	-	1099	57.6
1.5	44	1.56	1944	10.0	Thyratron	5.0	9.5	199	10.2
					Anode Assembly	2.0	11.1	93	4.8
					Cathode Assembly	2.0	11.8	98	5.0
					Tube Assembly	-	-	1554	80.0
		1.0	2090(2)	10.0	Thyratron	8.0	9.5	319	15.3
					Anode Assembly	3.5	11.1	163	7.8
					Cathode Assembly	2.5	11.8	123	5.9
					Tube Assembly	-	-	1485	71.0
		0.893	2217	9.0	Thyratron	3.0	22.2	233	10.5
					Anode Assembly	2.0	20.0	167	7.5
					Cathode Assembly	0.0	25.0	0	0.0
					Tube Assembly	-	-	1817	82.0

a) power into the tube assembly can vary from 60 to 80% of the power supply output thereby significantly impacting output performance;

b) losses in the window assembly account for about one half the losses;

c) losses in the thyratron account for the other half; and

d) there appears to be little dependence of laser PRF.

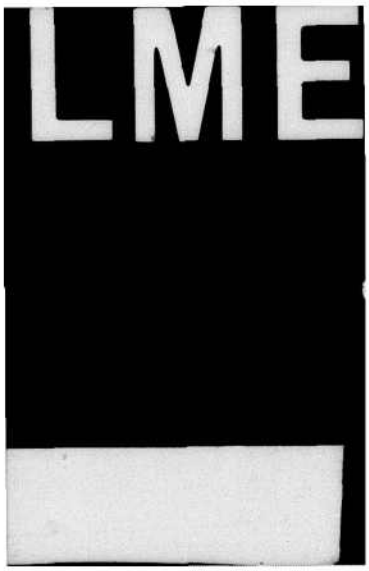
LME